

Figure 2. FK506 administration inhibited calcineurin activation and significantly attenuated development of cardiac hypertrophy in GCA-KO mice. A, Calcineurin activity in hearts of each group. B, FK506 administration partially, yet significantly, attenuated heart-to-body weight ratio (HW/BW) in GCA-KO mice. C, Representative images of M-mode echocardiograms. Data are expressed as mean \pm SEM of n=15 or 16 animals per group. * P <0.05 vs vehicle-treated WT; † P <0.05 vs vehicle-treated KO. Abbreviations are as defined in text.

significantly elevated in GCA-KO mice compared with WT. FK506 treatment strongly suppressed the expression of ANP and BNP in GCA-KO mice but had no effect in WT mice. Ventricular expression of collagen I, collagen III, and fibronectin was also significantly elevated in GCA-KO mice compared with WT. FK506 treatment strongly suppressed the expression of these genes in GCA-KO mice but had no effect in WT mice.

FK506 Attenuates GATA4 DNA-Binding Activity in GCA-KO Mice

Previous studies have demonstrated that GATA4 is involved in reactivation of the fetal gene program in response to a variety of hypertrophic stimuli and that NFAT may cooperate with GATA4 in the activation of hypertrophic gene markers.^{13,31} We therefore assessed whether GATA4 DNA-binding activity was enhanced in GCA-KO mice. The identity of the GATA4-specific band was confirmed by competition and supershift analyses with unlabeled oligonucleotide and anti-GATA4 antibody (Figure 6A). A representative EMSA with a GATA consensus oligonucleotide and quantitative analysis are shown in Figure 6B and 6C. GATA4 DNA-binding activity was significantly enhanced in GCA-KO mice

compared with WT. FK506 treatment strongly suppressed GATA4 DNA-binding activity in GCA-KO mice and mildly suppressed this activity in WT mice.

Inhibitory Regulation of the Calcineurin-NFAT Pathway by Locally Secreted Natriuretic Peptides in the Heart

We previously reported that endogenous natriuretic peptides inhibit cardiac myocyte hypertrophy in vitro with use of the natriuretic receptor antagonist HS-142-1.⁶ We therefore investigated whether locally secreted natriuretic peptides were able to inhibit the calcineurin-NFAT pathway in cardiac myocytes in an autocrine manner. As shown in Figure 7A, HS-142-1 significantly elevated calcineurin activity under basal (121% versus control) and PE-stimulated (125% versus PE) conditions. In addition, HS-142-1 significantly elevated *MC1P1* gene expression under basal (151% versus control) and PE-stimulated (130% versus PE) conditions (Figure 7B). Furthermore, we investigated whether HS-142-1 treatment was able to induce the translocation of cytoplasmic NFATc3 to the nucleus and whether exogenous ANP had an effect on NFATc3 translocation. As shown in Figure 7C, NFATc3 was detected in the cytoplasm of nearly all control cardiac

TABLE 1. Body Weight, SBP, and HR in Each Experimental Group

	WT+Vehicle		WT+FK506		KO+Vehicle		KO+FK506	
	10 wk	14 wk	10 wk	14 wk	10 wk	14 wk	10 wk	14 wk
BW, g	28.9 \pm 0.8	31.7 \pm 0.9	28.7 \pm 0.6	30.8 \pm 0.7	29.5 \pm 0.5	32.3 \pm 0.7	30.4 \pm 0.7	33.1 \pm 0.7
SBP, mmHg	100.6 \pm 1.7	104.4 \pm 1.7	99.7 \pm 1.4	101.5 \pm 1.8	136.3 \pm 1.8*	136.9 \pm 1.0†	134.6 \pm 1.8‡	132.4 \pm 3.7§
HR, bpm	616 \pm 6	620 \pm 5	618 \pm 7	609 \pm 10	615 \pm 7	618 \pm 5	620 \pm 6	619 \pm 2

BW indicates body weight. Data are expressed as mean \pm SEM. n=15 or 16.

* P <0.05 vs vehicle-treated WT at 10 weeks.

† P <0.05 vs vehicle-treated WT at 14 weeks.

‡ P <0.05 vs FK506-treated WT at 10 weeks.

§ P <0.05 vs FK506-treated WT at 14 weeks.

TABLE 2. Echocardiographic Characteristics in Each Experimental Group

	WT+Vehicle	WT+FK506	KO+Vehicle	KO+FK506
IVSth, mm	0.55±0.02	0.54±0.02	0.87±0.05*	0.66±0.02†
LVPWth, mm	0.57±0.03	0.56±0.03	0.92±0.05*	0.68±0.02†
LVDd, mm	3.88±0.05	3.76±0.07	4.31±0.08*	3.94±0.08†
LVDs, mm	2.46±0.07	2.42±0.06	2.60±0.07	2.44±0.07
FS, %	37.2±1.3	35.7±1.3	39.7±1.4	38.1±1.6
HR, bpm	268±12	272±13	262±9	279±11

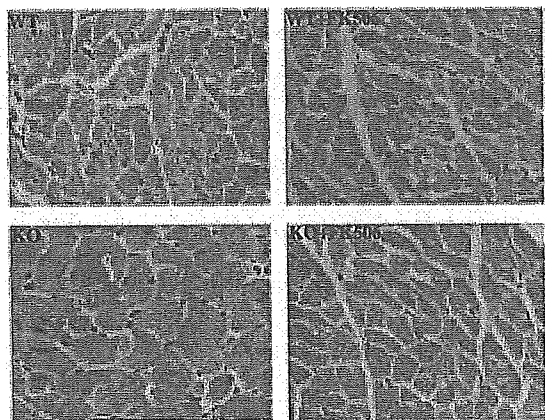
LVDs indicates left ventricular end-systolic diameter; FS, fractional shortening. n=15 or 16.

* $P<0.05$ vs vehicle-treated WT.

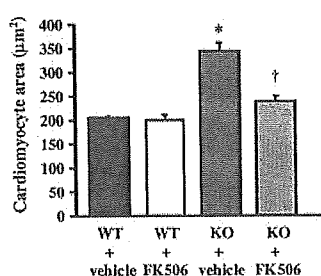
† $P<0.05$ vs vehicle-treated KO.

myocytes. However, treatment of cardiac myocytes with HS-142 (100 $\mu\text{g}/\text{mL}$) induced the nuclear translocation of NFATc3 (Figure 7D). PE (10^{-6} mol/L) stimulation also caused the nuclear translocation of NFATc3 (Figure 7E). However, pretreatment of cardiac myocytes with ANP (10^{-6} mol/L) prevented PE-induced NFATc3 translocation (Figure 7F). In addition, pretreatment of cardiac myocytes with the cyclic GMP analog 8-bromo-cyclic GMP (10^{-3} mol/L) also inhibited PE-induced NFATc3 translocation (Figure 7G). GATA4 was stably detected in the nucleus under all experimental conditions.

A



B



C

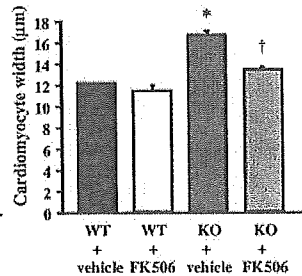
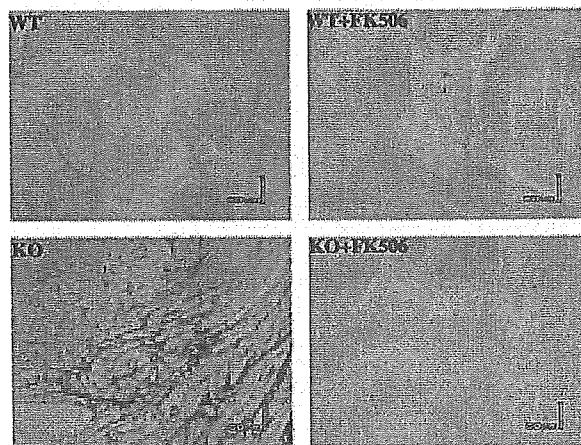


Figure 3. A, Effects of FK506 administration on cardiac myocyte hypertrophy in GCA-KO mice. A, Representative photomicrographs of cardiomyocyte size in sections stained with hematoxylin and eosin ($\times 400$ magnification). B, Quantitative morphometric analysis of cardiomyocyte area. C, Quantitative morphometric analysis of cardiomyocyte width. * $P<0.05$ vs vehicle-treated WT; † $P<0.05$ vs vehicle-treated KO. Abbreviations are as defined in text.

A



B

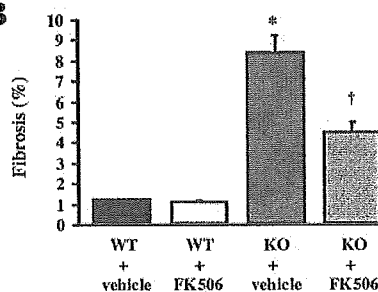


Figure 4. Effects of FK506 administration on cardiac fibrosis in GCA-KO mice. A, Representative photomicrographs of collagen volume fraction in sections stained with Sirius red ($\times 200$ magnification). B, Quantitative morphometric analysis of cardiac fibrosis. Data are expressed as mean \pm SEM of n=7 or 8 animals per group. * $P<0.05$ vs vehicle-treated WT; † $P<0.05$ vs vehicle-treated KO. Abbreviations are as defined in text.

Discussion

This study has demonstrated for the first time that disruption of the GCA gene results in activation of the cardiac calcineurin-NFAT pathway. Moreover, pharmacological blockade of calcineurin activity markedly inhibited cardiac hypertrophy and fibrosis in GCA-KO mice. We have also demonstrated that blockade of endogenous GCA induces activation of the calcineurin-NFAT pathway in cultured cardiac myocytes.

As has been reported previously, GCA plays a primary role in moderating cardiac hypertrophy in vivo, independent of its effects on BP regulation.^{10–12} However, which intracellular signaling pathway contributes to GCA-mediated inhibition of cardiac hypertrophy has not been elucidated. Recent studies have recognized the importance of the calcineurin-NFAT signaling pathway in cardiac growth. Molkenin et al¹³ and Vega et al¹⁴ showed that cardiac hypertrophy was induced by the calcium-dependent phosphatase calcineurin, which dephosphorylates the transcription factor NFAT, enabling it to translocate to the nucleus. NFAT then interacts with the zinc finger transcription factor GATA4 and synergistically activates cardiac embryonic gene reprogramming.^{13,14} Therefore, it is tempting to speculate that GCA exerts its antihypertrophic action by antagonizing the calcineurin-NFAT pathway. However, the role of endogenous GCA in the regulation of the calcineurin-NFAT pathway has not been elucidated.

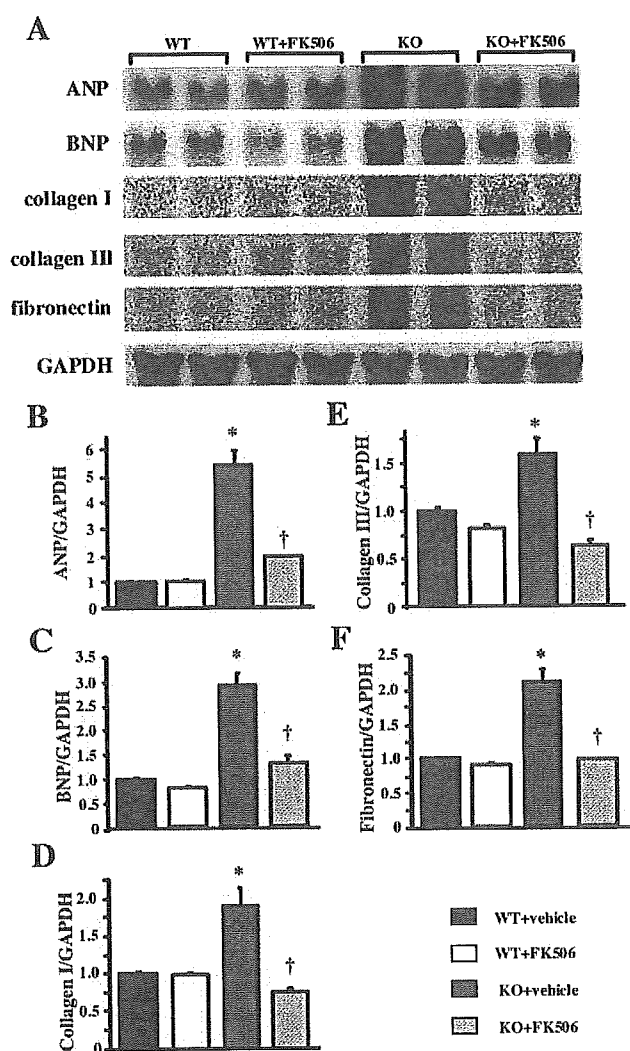


Figure 5. Calcineurin activation was involved in increased mRNA expression associated with cardiac remodeling in GCA-KO mice. A, Representative images of Northern blots of ANP, BNP, collagen type I, collagen type III, fibronectin, and GAPDH mRNAs in heart. B–F, Quantitative analysis of expression of each gene. In individual samples, each mRNA value was corrected for GAPDH mRNA. Expression levels in vehicle-treated WT mice were arbitrarily assigned value of 1.0. Data are expressed as mean ± SEM of n=7 or 8 animals per group. * $P < 0.05$ vs vehicle-treated WT; † $P < 0.05$ vs vehicle-treated KO. Abbreviations are as defined in text.

Therefore, in this study, we investigated the significance of the calcineurin-NFAT pathway in cardiac remodeling in mice deficient for GCA. We found that calcineurin activity, NFATc3 translocation to the nucleus, and *MC1P1* gene expression were upregulated in the absence of GCA. In addition, chronic pharmacological inhibition of calcineurin by FK506 administration suppressed cardiac hypertrophy and fibrosis. FK506 attenuated not only cardiac hypertrophy but also cardiac dilation without affecting cardiac contractility. Moreover, the cross-sectional areas and widths of cardiac myocytes and interstitial fibrosis, which were significantly increased in GCA-KO mice, were all attenuated by FK506 treatment. Marked increases in ventricular expression of the genes for ANP, BNP, collagen I, collagen III, and fibronectin

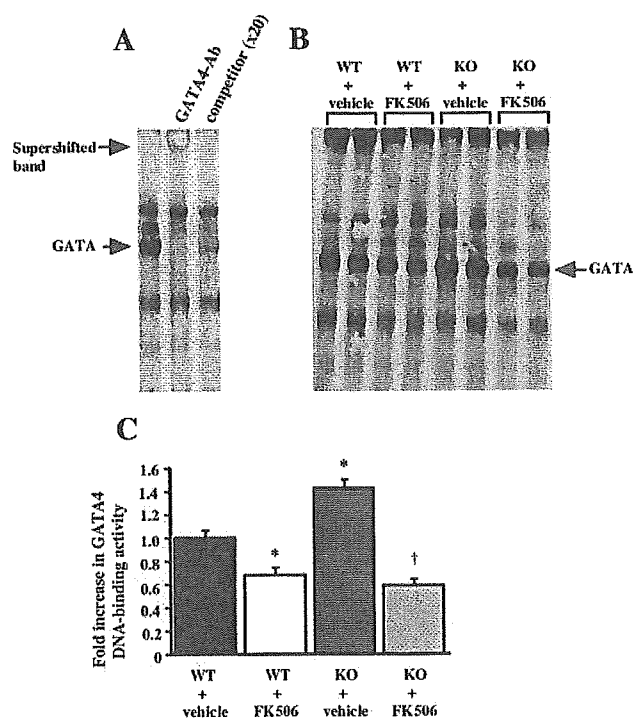


Figure 6. GATA4 DNA-binding activity was increased in GCA-KO mice. FK506 administration suppressed increased activation. A, Identification of band obtained in GATA gel-shift assay was confirmed by supershift assay with anti-GATA4 antibody and by specific (unlabeled GATA consensus oligonucleotide) competition. B, Representative EMSA with GATA consensus oligonucleotide and lysates from vehicle-treated WT, FK506-treated WT, vehicle-treated KO, and FK506-treated KO mice. C, Quantitative analysis of EMSA with GATA consensus oligonucleotide in each animal group. Data are expressed as mean ± SEM of n=4 animals per group. * $P < 0.05$ vs vehicle-treated WT; † $P < 0.05$ vs vehicle-treated KO. Abbreviations are as defined in text.

were observed in GCA-KO mice; these effects were significantly attenuated by FK506 treatment. GATA4 is a transcriptional regulator of the hypertrophic response and cooperates with NFAT to activate the BNP promoter in cardiac myocytes.^{13,31} In this study, we have demonstrated that GATA4 DNA-binding activity was augmented in GCA-KO mice and that FK506 treatment diminished this activity. Taken together, these results suggest that activation of the calcineurin-NFAT pathway and the subsequent activation of GATA4 play an important role in cardiac hypertrophy and fibrosis in GCA-KO mice.

Although the calcineurin-NFAT pathway was activated in GCA-KO mice, the upstream factor(s) that activates the calcineurin-NFAT pathway has not been identified. We suggest that the renin-angiotensin (Ang) II system may contribute to calcineurin activation in GCA-KO mice. We previously reported that targeted deletion or pharmacological blockade of the Ang II type 1A receptor ameliorated cardiac hypertrophy and interstitial fibrosis in GCA-KO mice.³² Furthermore, it has been reported that a nonantihypertensive dose of the selective Ang II type 1A receptor blocker candesartan attenuated cardiac calcineurin activity and the development of cardiac hypertrophy and fibrosis in hyperten-

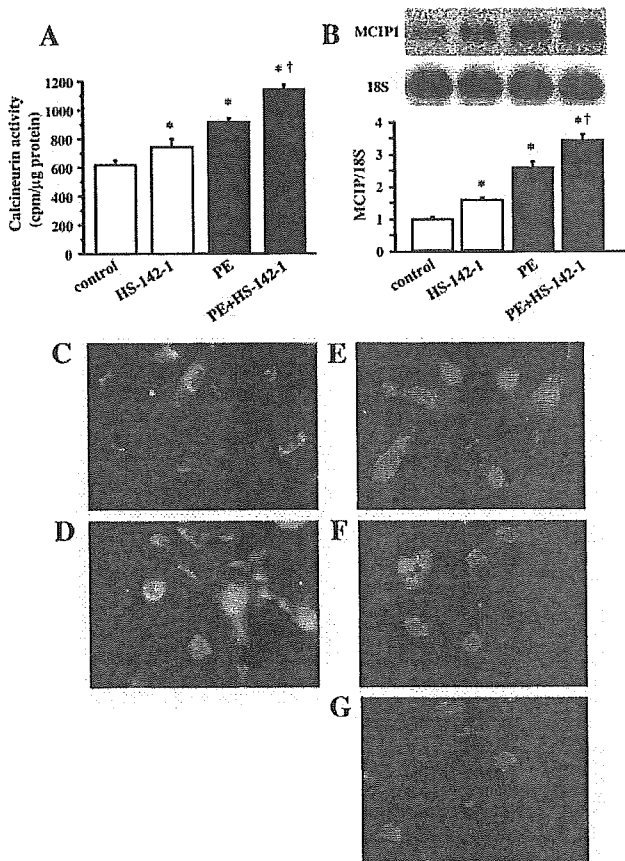


Figure 7. A, HS-142-1 (100 $\mu\text{g}/\text{mL}$) treatment significantly elevated calcineurin activity in cultured cardiac myocytes under nonstimulated (open bars) and PE (10^{-6} mol/L)-stimulated (solid bars) conditions. Cells were preincubated in presence or absence of HS-142-1 for 1 hour and then incubated in presence or absence of PE for 2 minutes. Values are mean \pm SEM of 4 measurements. * $P < 0.05$ vs control; † $P < 0.05$ vs PE alone. B, HS-142-1 (100 $\mu\text{g}/\text{mL}$) treatment significantly elevated *MCIP1* gene expression in cultured cardiac myocytes under nonstimulated (open bars) and PE (10^{-6} mol/L)-stimulated (solid bars) conditions. Cells were incubated for 24 hours in presence or absence of HS-142-1 and/or PE. Representative images of Northern blot and quantitative analysis are shown. Values shown were corrected with density of corresponding 18S ribosomal RNA. Data are mean \pm SEM of 4 measurements. * $P < 0.05$ vs control; † $P < 0.05$ vs PE alone. C–G, HS-142-1 (100 $\mu\text{g}/\text{mL}$) treatment caused translocation of NFATc3 into nucleus. Cells were incubated for 12 hours in absence (C) or presence (D) of HS-142-1 (100 $\mu\text{g}/\text{mL}$), PE (10^{-6} mol/L), E, PE (10^{-6} mol/L) plus ANP (10^{-6} mol/L, F), or PE (10^{-6} mol/L) plus 8-bromo-cyclic GMP (10^{-3} mol/L, G). Cells were then subjected to immunofluorescence with anti-NFATc3 and anti-GATA4 antibodies. Abbreviations are as defined in text.

sive rats.²³ This suggests that GCA inhibits calcineurin activity at least in part by interacting with Ang II signaling. However, other factors are probably involved in calcineurin activation in GCA-KO mice, because targeted deletion or pharmacological blockade of the Ang II type 1A receptor significantly reduced, but did not completely inhibit, cardiac remodeling in GCA-KO mice.³²

Because we cannot exclude the involvement of high BP in calcineurin activation in GCA-KO mice, we next examined whether locally secreted natriuretic peptides/GCA signaling was able to directly inhibit the calcineurin-NFAT pathway in

an autocrine manner by using HS-142-1, a natriuretic receptor antagonist, in cultured cardiac myocytes. Treatment with HS-142-1 increased calcineurin activity and *MCIP1* gene expression under both basal and PE-stimulated conditions. Furthermore, HS-142-1 induced the nuclear translocation of NFATc3. These in vitro results confirm that inhibition of GCA leads to activation of the calcineurin pathway. Importantly, a cyclic GMP analog and exogenous ANP both inhibited PE-induced nuclear translocation of NFATc3. Because ANP- or BNP-induced activation of GCA leads to an increase in intracellular cyclic GMP levels,³³ GCA-mediated inhibition of the calcineurin-NFAT pathway might occur in part through activation of cyclic GMP and its effectors. In fact, Fiedler et al³⁴ recently demonstrated in vitro that cyclic GMP-dependent protein kinase inhibits calcineurin-NFAT signaling upstream of calcineurin and may also inhibit the pathway downstream of calcineurin. In addition, we previously reported that blockade of endogenous natriuretic peptides induced hypertrophy in cultured cardiac myocytes, probably via a cyclic GMP-dependent mechanism.⁶ Taken together, these results suggest that ANP or BNP may play a role as an autocrine factor in the regulation of cardiac myocyte hypertrophy, in part via cyclic GMP-dependent protein kinase-mediated inhibition of the calcineurin-NFAT pathway. A schematic diagram depicting the signaling supported by the present study is shown in Figure 8.

Although inhibition of calcineurin attenuated cardiac fibrosis and markers of fibrosis in this study, the mechanism underlying these observations is not yet well understood. Transforming growth factor (TGF)- β 1 is a potent stimulator of extracellular matrix protein synthesis (eg, collagen and fibronectin).³⁵ We previously reported that *TGF- β 1* gene expression is significantly increased in the hearts of GCA-KO mice.³² Recently, the involvement of calcineurin in TGF- β -mediated regulation of extracellular matrix accumulation in other cell types has been reported.³⁶ Therefore, inhibition of TGF- β 1 signaling in cardiac fibroblasts might be one mechanism whereby FK506 treatment induces attenuation of cardiac fibrosis.

In the present study, the inhibitory effect of FK506 treatment on cardiac hypertrophy was more potent than on cardiac fibrosis. Although the exact mechanisms are unknown, the calcineurin pathway might be differently activated depending on cell type. In fact, *MCIP* expression, which is regulated by calcineurin activation, was observed primarily in cardiac myocytes.

It has recently been suggested that various signaling molecules coordinate with the calcineurin-NFAT pathway. The involvement of mitogen-activated protein kinase (MAPK) pathways, including c-Jun-NH₂-terminal kinase (JNK), extracellular regulated kinase (ERK), and P38 MAPK, have been well characterized in cardiac hypertrophy.³⁷ However, it had been reported that the activities of JNK, ERK, and P38 MAPK were not activated in GCA-KO mice.¹⁰ Further investigations are necessary to identify effectors that play a role in the enhanced cardiac hypertrophy observed in GCA-KO mice.

In the present study, the HR of mice during echocardiography was lower than that observed in conscious mice. In fact,

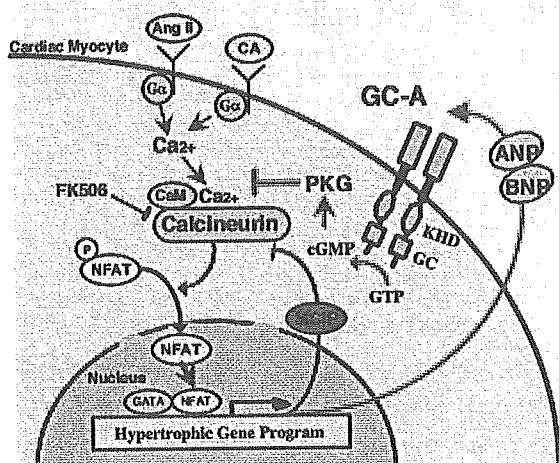


Figure 8. Interactions between GCA and calcineurin signaling pathways suggested from findings of present and previous studies. Neuroendocrine factors stimulate G protein-coupled receptors (GPCRs). GPCRs are typically coupled to G proteins, which lead to elevation of intracellular Ca^{2+} and activation of calmodulin-regulated phosphatase, calcineurin. Calcineurin activation causes nuclear localization of NFAT transcription factors by dephosphorylation. NFAT and GATA4 cooperatively activate transcription of hypertrophic gene program, including ANP and BNP genes. MCIP gene is also target of NFAT and is upregulated in response to calcineurin signaling. MCIP has been proposed to create negative-feedback loop that suppresses calcineurin activity. In present study, we suggested possibility that endogenous ANP and BNP mediate antihypertrophic effects through GCA/cGMP/PKG signaling, which inhibits calcineurin-NFAT pathway. ANP and BNP may also create negative-feedback loop that suppress calcineurin activity. However, how GCA/cGMP/PKG signaling mediates calcineurin inhibition is unclear. CA indicates catecholamine; CaM, calmodulin; KHD, kinase-homology regulatory domain; GC, GC catalytic domain; and PK, protein kinase. Other abbreviations are as defined in text.

acutely during anesthesia, a combination of ketamine and xylazine is known to decrease HR, left ventricular systolic pressure, and maximal dp/dt .³⁸ Although there was no significant difference in HR between any of the mouse groups (Table 2), suggesting that the depths of anesthesia were similar, some of the echocardiographic comparisons could be either accentuated or obscured by prolongation of filling time and/or inhibition of cardiac function because of the effects of anesthesia.

Nakayama et al³⁹ previously described a functional mutation in the 5'-flanking region of the human *GCA* gene that is associated with essential hypertension and cardiac hypertrophy. *GCA* gene expression is most likely diminished in these patients because of the mutation, predisposing them to cardiac hypertrophy and fibrosis like that seen in *GCA-KO* mice. The results reported herein suggest that inhibition of the calcineurin-NFAT pathway would be the treatment of choice to prevent cardiac hypertrophy and fibrosis in patients with lower expression of *GCA*.

In conclusion, our results indicate that activation of the calcineurin-NFAT pathway is intimately involved in cardiac remodeling of *GCA-KO* mice. These findings offer new

insight into endogenous mechanisms for protection of the heart by natriuretic peptides/*GCA* signaling.

Acknowledgments

This study was supported by the Program for Promotion of Fundamental Studies in Health Sciences of the Pharmaceuticals and Medical Devices Agency; research grants from the Japanese Ministry of Education, Science, and Culture; and the Japanese Ministry of Health, Labor and Welfare. We thank Chika Fukuhara for excellent technical assistance.

References

1. Nakao K, Itoh H, Saito Y, Mukoyama M, Ogawa Y. The natriuretic peptide family. *Curr Opin Nephrol Hypertens*. 1996;5:4–11.
2. Kishimoto I, Garbers DL. Physiological regulation of blood pressure and kidney function by guanylyl cyclase isoforms. *Curr Opin Nephrol Hypertens*. 1997;6:58–63.
3. Lin X, Hänze J, Heese F, Sodmann R, Lang RE. Gene expression of natriuretic peptide in myocardial cells. *Circ Res*. 1995;77:750–758.
4. Horio T, Tokudome T, Maki T, Yoshihara F, Suga S, Nishikimi T, Kojima M, Kawano Y, Kangawa K. Gene expression, secretion, and autocrine action of C-type natriuretic peptide in cultured adult rat cardiac fibroblasts. *Endocrinology*. 2003;144:2279–2284.
5. Tokudome T, Horio T, Soeki T, Mori K, Kishimoto I, Suga S, Yoshihara F, Kawano Y, Kohno M, Kangawa K. Inhibitory effect of C-type natriuretic peptide (CNP) on cultured cardiac myocyte hypertrophy: interference between CNP and endothelin-1 signaling pathways. *Endocrinology*. 2004;145:2131–2140.
6. Horio T, Nishikimi T, Yoshihara T, Matsuo H, Takishita S, Kangawa K. Inhibitory regulation of hypertrophy by endogenous atrial natriuretic peptide in cultured cardiac myocytes. *Hypertension*. 2000;35:19–24.
7. Lopez MJ, Wong SK, Kishimoto I, Dubois S, Mach V, Friesen J, Garbers DL, Beuve A. Salt-resistant hypertension in mice lacking the guanylyl cyclase-A receptor for atrial natriuretic peptide. *Nature*. 1995;378:65–68.
8. Oliver PM, Fox JE, Kim R, Rockman HA, Kim HS, Reddick RT, Pandey KN, Milgram SL, Smithies O, Maeda N. Hypertension, cardiac hypertrophy, and sudden death in mice lacking natriuretic peptide receptor A. *Proc Natl Acad Sci U S A*. 1997;94:14730–14735.
9. Garbers DL, Dubois SK. The molecular basis of hypertension. *Annu Rev Biochem*. 1999;68:127–155.
10. Knowles JW, Esposito G, Mao L, Hagaman JR, Fox JE, Smithies O, Rockman HA, Maeda N. Pressure-independent enhancement of cardiac hypertrophy in natriuretic peptide receptor A-deficient mice. *J Clin Invest*. 2001;107:975–984.
11. Kishimoto I, Rossi K, Garbers DL. A genetic model provides evidence that the receptor for atrial natriuretic peptide (guanylyl cyclase-A) inhibits cardiac ventricular myocyte hypertrophy. *Proc Natl Acad Sci U S A*. 2001;98:2703–2706.
12. Holtwick R, Eickels MV, Skryabin BV, Baba HA, Bubikat A, Begrow F, Schneider MD, Garbers DL, Kuhn M. Pressure-independent cardiac hypertrophy in mice with cardiomyocyte-restricted inactivation of the atrial natriuretic peptide receptor guanylyl cyclase-A. *J Clin Invest*. 2003;111:1399–1407.
13. Molkenin JD, Lu JR, Antos CL, Markham B, Richardson J, Robbins J, Grant SR, Olson EN. A calcineurin-dependent transcriptional pathway for cardiac hypertrophy. *Cell*. 1998;93:215–228.
14. Vega RB, Bassel-Duby R, Olson EN. Control of cardiac growth and function by calcineurin signaling. *J Biol Chem*. 2003;278:36981–36984.
15. Klee CB, Ren H, Wang X. Regulation of the calmodulin-stimulated protein phosphatase, calcineurin. *J Biol Chem*. 1998;273:13367–13370.
16. Crabtree GR. Calcium, calcineurin, and the control of transcription. *J Biol Chem*. 2001;276:2313–2316.
17. Dolmetsch RE, Lewis RS, Goodnow CC, Healy JJ. Differential activation of transcriptional factors induced by Ca^{2+} response amplitude and duration. *Nature*. 1997;386:855–858.
18. Molkenin JD. Calcineurin and beyond: cardiac hypertrophic signaling. *Circ Res*. 2000;87:731–738.
19. Shimoyama M, Hayashi D, Zou Y, Takimoto E, Mizukami M, Monzen K, Kudoh S, Hiroi Y, Yazaki Y, Nagai R, Komuro I. Calcineurin inhibitor attenuates the development and induces the regression of cardiac hypertrophy in rats with salt-sensitive hypertension. *Circulation*. 2000;102:1996–2004.

20. Sakata Y, Masuyama T, Yamamoto K, Nishikawa N, Yamamoto H, Kondo H, Ono K, Otsu K, Kuzuya T, Miwa T, Takeda H, Miyamoto E, Hori M. Calcineurin inhibitor attenuates left ventricular hypertrophy, leading to prevention of heart failure in hypertensive rats. *Circulation*. 2000;102:2269–2275.
21. Zou Y, Hiroi Y, Uozumi H, Takimoto E, Toko H, Zhu W, Kudoh S, Mizukami M, Shimoyama M, Shibasaki F, Nagai R, Yazaki Y, Komuro I. Calcineurin plays a critical role in the development of pressure overload-induced cardiac hypertrophy. *Circulation*. 2001;104:97–101.
22. Takeda Y, Yoneda T, Demura M, Usukura M, Mabuchi H. Calcineurin inhibition attenuates mineralocorticoid-induced cardiac hypertrophy. *Circulation*. 2002;105:677–679.
23. Nagata K, Somura F, Obata K, Odashima M, Izawa H, Ichihara S, Nagasaka T, Iwase M, Yamada Y, Nakashima N, Yokota M. AT₁ receptor blockade reduces cardiac calcineurin activity in hypertensive rats. *Hypertension*. 2002;40:168–174.
24. Blumenthal DK, Takio K, Hansen RS, Krebs EG. Dephosphorylation of cAMP-dependent protein kinase regulatory subunit (type II) by calmodulin-dependent protein phosphatase. *J Biol Chem*. 1986;261:8140–8145.
25. Fruman DA, Klee CB, Bierer BE, Burakoff SJ. Calcineurin phosphatase activity in T lymphocytes is inhibited by FK506 and cyclosporin A. *Proc Natl Acad Sci U S A*. 1992;89:3686–3690.
26. Zheng JS, Boluyt MO, O'Neill L, Crow MT, Lakatta EG. Extracellular ATP induces immediate-early gene expression but not cellular hypertrophy in neonatal cardiac myocytes. *Circ Res*. 1994;74:1034–1041.
27. Harada M, Itoh H, Nakagawa O, Ogawa Y, Miyamoto Y, Kuwahara K, Ogawa E, Igaki T, Yamashita J, Masuda I, Yoshimasa T, Tanaka I, Saito Y, Nakao K. Significance of ventricular myocytes and nonmyocytes interaction during cardiocyte hypertrophy: evidence for endothelin-1 as a paracrine hypertrophic factor from cardiac nonmyocytes. *Circulation*. 1997;96:3737–3744.
28. Wilkins BJ, De Windt LJ, Bueno OF, Braz JC, Glascock BJ, Kimball TF, Molkentin JD. Targeted disruption of NFATc3, but not NFATc4, reveals an intrinsic defect in calcineurin-mediated cardiac hypertrophic growth. *Mol Cell Biol*. 2002;22:7603–7613.
29. Thibault G, Amiri F, Garcia R. Regulation of natriuretic peptide secretion by the heart. *Annu Rev Physiol*. 1999;61:193–217.
30. De Bold AJ, Bruneau BG, Kuroski de Bold ML. Mechanical and neuroendocrine regulation of the endocrine heart. *Cardiovasc Res*. 1996;31:7–18.
31. Molkentin JD, Olson EN. GATA4: a novel transcriptional regulator of cardiac hypertrophy? *Circulation*. 1997;96:3833–3835.
32. Li Y, Kishimoto I, Saito Y, Harada M, Kuwahara K, Izumi T, Takahashi N, Kawakami R, Tanimoto K, Nakagawa Y, Nakanishi M, Adachi Y, Garbers DL, Fukamizu A, Nakao K. Guanylyl cyclase-A inhibits angiotensin II type 1A receptor-mediated cardiac remodeling, an endogenous protective mechanism in the heart. *Circulation*. 2002;106:1722–1728.
33. Kuhn M. Structure, regulation, and function of mammalian membrane guanylyl cyclase receptors, with a focus on guanylyl cyclase-A. *Circ Res*. 2003;93:700–709.
34. Fiedler B, Lohmann SM, Smolenski A, Linnemüller S, Pieske B, Schröder F, Molkentin JD, Drexler H, Wollert KC. Inhibition of calcineurin-NFAT hypertrophy signaling by cGMP-dependent protein kinase type I in cardiac myocytes. *Proc Natl Acad Sci U S A*. 2002;99:11363–11368.
35. Weber KT, Brilla CG. Pathological hypertrophy and cardiac interstitium: fibrosis and renin-angiotensin-aldosterone system. *Circulation*. 1991;83:1849–1865.
36. Gooch JL, Gorin Y, Zhang BX, Abboud HE. Involvement of calcineurin in transforming growth factor- β -mediated regulation of extracellular matrix accumulation. *J Biol Chem*. 2004;279:15561–15570.
37. Ravingerova T, Barancik M, Strniskova M. Mitogen-activated protein kinases: a new therapeutic target in cardiac pathology. *Mol Cell Biochem*. 2003;247:127–138.
38. Ishizuka S, Sievers RE, Zhu BQ, Rodrigo MC, Joho S, Foster E, Simpson PC, Grossman W. New technique for measurement of left ventricular pressure in conscious mice. *Am J Physiol Heart Circ Physiol*. 2004;286:H1208–H1215.
39. Nakayama T, Soma M, Takahashi Y, Rehemudula D, kamatsuse K, Furuya K. Functional deletion mutation of the 5'-flanking region of type A human natriuretic peptide receptor gene and its association with essential hypertension and left ventricular hypertrophy in the Japanese. *Circ Res*. 2000;86:841–845.

Primary Hyperparathyroidism Presumably Caused by Chronic Parathyroiditis Manifesting from Hypocalcemia to Severe Hypercalcemia

Sumiko FURUTO-KATO, Shigeru MATSUKURA, Makoto OGATA, Nobuyuki AZUMA, Toshiaki MANABE*, Chohei SHIGENO**, Ryo ASATO***, Kiyoshi TANAKA****, Yasato KOMATSU***** and Kazuwa NAKAO*****

Abstract

A 67-year-old woman who presented with hypocalcemia compatible with idiopathic hypoparathyroidism gradually changed into a state of primary hyperparathyroidism. The left upper parathyroid gland, which was larger and harder than other glands, was resected. Despite the operation, hypercalcemia and high levels of intact PTH persisted. Six weeks later total parathyroidectomy was done to induce remission. The resected gland in the first operation had clusters of lymphoid follicles with germinal centers indicating a chronic autoimmune inflammation. This case suggests a transition from hypoparathyroidism to hyperparathyroidism associated with chronic parathyroiditis, possibly by a mechanism analogous to that observed in chronic thyroiditis. (*Internal Medicine* 44: 60–64, 2005)

Key words: hyperparathyroidism, chronic parathyroiditis, lymphoid follicles with germinal centers, hypercalcemia, hypocalcemia, Hashimoto's disease

Introduction

Primary hyperparathyroidism is generally caused by parathyroid adenoma, hyperplasia or occasionally carcinoma. The cause of hyperparathyroidism without the above lesions is sometimes difficult to identify. Regarding the pathology of the parathyroid gland, lymphoid follicles with germinal cen-

ters are rarely present in the parathyroid tissues. The presence of lymphoid follicles may indicate a chronic inflammatory process in the tissue. Bondeson et al (1) first reported two cases of chronic parathyroiditis associated with hyperparathyroidism. The possibility of hyperparathyroidism caused by autoimmunity in the parathyroid gland in the context of Graves' disease-like lymphoid infiltrate has been postulated. Since there was no evidence of underlying infections, a developmental anomaly, or drug reactions that could explain the inflammatory component, they suggested that an autoimmune process may have been involved in the pathogenesis (1). Chronic parathyroiditis itself has rarely been reported to date. Furthermore, cases manifesting severe hypocalcemia later changing to severe hypercalcemia associated with chronic parathyroiditis have not been reported to our knowledge. We report here a rare case of primary hyperparathyroidism which was presumably due to chronic parathyroiditis, which manifested from hypocalcemia to severe hypercalcemia.

Case Report

A 67-year-old woman saw a home doctor because of finger numbness in January 2000. She was referred to our hospital because plasma Ca levels were 6.4 mg/dl. When she visited our hospital on February 23, 2000, her plasma Ca and P levels were 7.2 mg/dl and 7.0 mg/dl, respectively. Plasma intact parathyroid hormone (PTH) was less than 9 pg/ml; the threshold of the assay. Her height was 159.2 cm, and her weight was 48.4 kg. Her blood pressure was 143/84 mmHg. In terms of family history her sister died of cerebral bleed-

From the Metabolism and Endocrinology Division of Internal Medicine, Kishiwada City Hospital, Osaka, *Department of Pathology, Kyoto University Graduate School of Medicine, Kyoto, **Department of Radiology, JT Kyoto Senbai Hospital, Kyoto, ***Department of Otolaryngology-Head and Neck Surgery, Kyoto University Graduate School of Medicine, Kyoto, ****Department of Nutrition, Kyoto Women University, Kyoto and *****Department of Medicine and Clinical Science, Kyoto University Graduate School of Medicine, Kyoto

Received for publication February 2, 2004; Accepted for publication August 17, 2004

Reprint requests should be addressed to Dr. Sumiko Furuto-Kato, the Metabolism and Endocrinology Division of Internal Medicine, Kishiwada City Hospital, 1001 Gakuhara-cho, Kishiwada, Osaka 596-8501

Chronic Parathyroiditis Manifesting Hypocalcemia to Hypercalcemia

ing, and she had had lung tuberculosis at 10 years of age. Physical examination on admission showed Chvostek sign and Trousseau sign, although the finger numbness had already disappeared. Laboratory data on admission on March 23, 2000 are summarized in Table 1. The results of Ellsworth-Howard test were compatible with idiopathic hypoparathyroidism. Other basal levels of hormones, with

the exception of PTH, were within normal limits. Treatment with $1\alpha, 25\text{-(OH)}_2\text{D}_3$ 2 $\mu\text{g}/\text{day}$ was initiated.

Plasma Ca and intact PTH gradually increased. The clinical course is shown in Fig. 1. Treatment with $1\alpha, 25\text{-(OH)}_2\text{D}_3$ was slowly tapered, then terminated. On November 13, 2000, plasma Ca and also intact PTH levels continued to increase without any treatment. In March 2001, both plasma Ca and intact PTH were above the normal upper limits. According to these state of parathyroid function, the clinical diagnosis was changed to primary hyperparathyroidism. Plasma Ca and intact PTH still increased slowly and consistently over the next several months, and six months after the diagnosis of primary hyperparathyroidism, an acute increase in plasma Ca levels occurred, peaking from 14.7 mg/dl to 16.5 mg/dl in September 2001 (Fig. 1). The patient suffered from severe fatigue, appetite loss and body weight loss of 9 kg, compatible with parathyroid crisis. A series of tests including an ultrasound echogram, $^{99\text{m}}\text{Tc-MIBI/I-123}$ subtraction scintigraphy, magnetic resonance imaging (MRI), and computed tomography (CT) of the neck and the chest could not provide any information regarding localization of the causative lesions. Plasma PTH-related protein (PTHrP)

Table 1. Ca Related Data on First Admission

Plasma Ca	6.5 mg/dl (8.6–10.6)
Plasma P	6.9 mg/dl (2.5–4.8)
Plasma Mg	1.9 mg/dl (1.5–2.8)
Ionized Ca	1.68 mEq/l (2.41–2.71)
24h urine Ca	0.03 g
24h urine Mg	0.05 g
Intact-PTH	13 pg/ml (10–65)
HS-PTH	200 pg/ml (160–520)
C-PTH	0.2 ng/ml (<0.5)
$1,25\text{-(OH)}_2$ Vitamin D	45.7 pg/ml (20–60)

(): normal range.

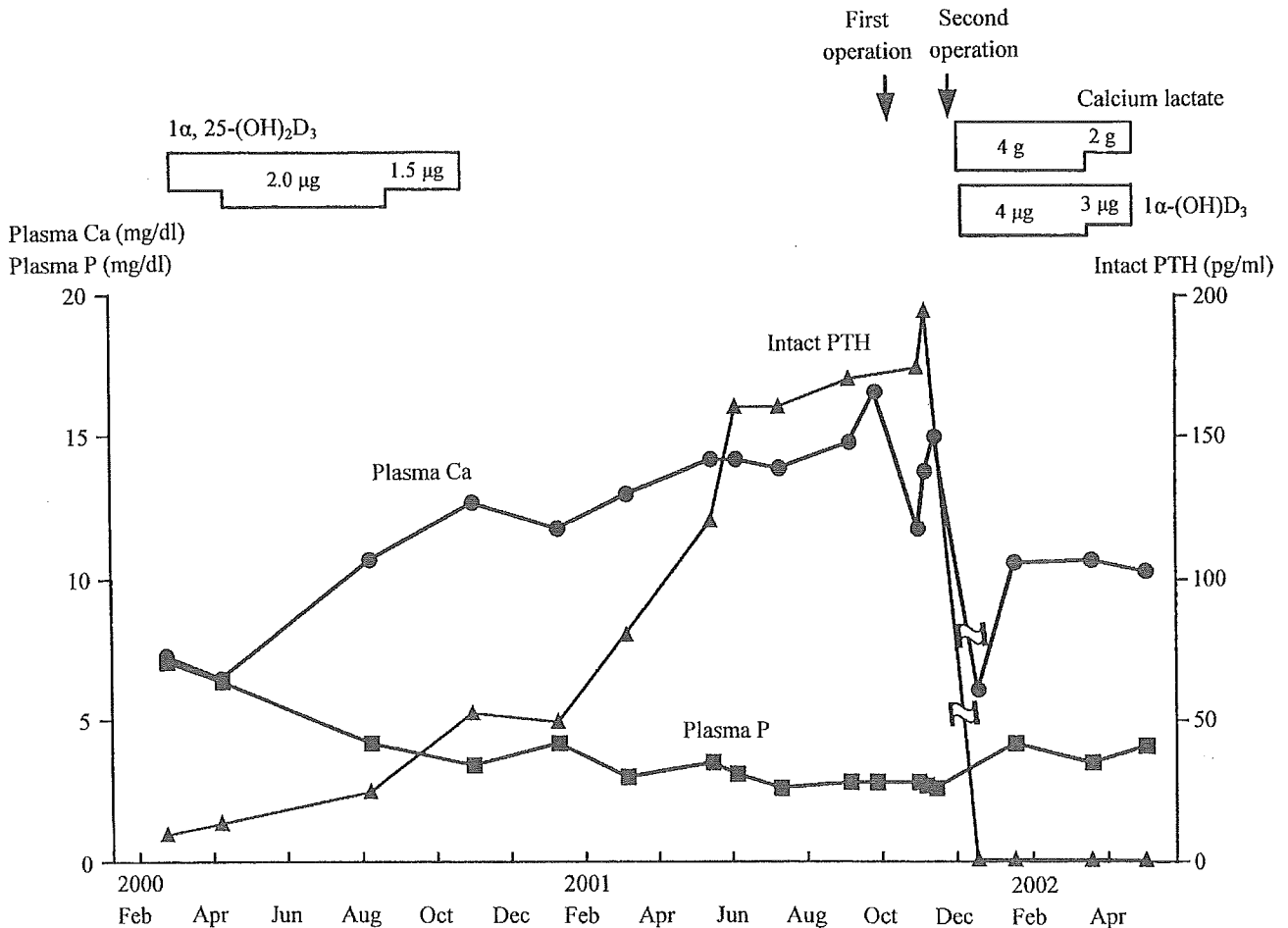


Figure 1. Clinical course of the patient.

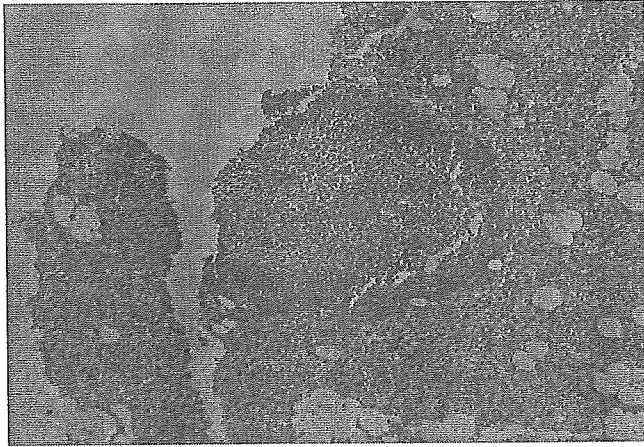


Figure 2. Pathology of left superior parathyroid gland extirpated at the first operation demonstrating lymphoid follicles containing germinal centers.

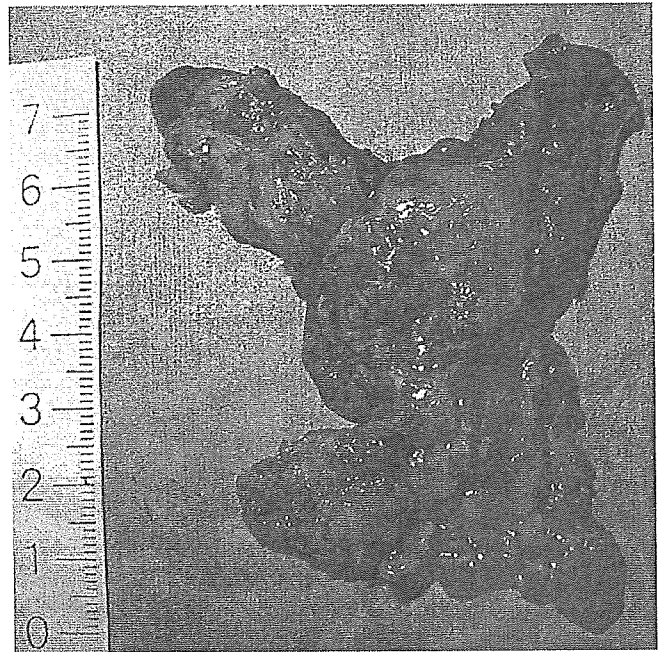


Figure 3. Resected specimens of the thyroid and fat tissue in the neck and superior thoracic region.

was within normal ranges. Antibodies against parathyroid gland and calcium-sensing receptor were not measured in the present study.

A parathyroidectomy was done on October 29, 2001. The left upper parathyroid gland, which was larger and harder than the other glands, was resected. Intraoperative frozen section showed that it was compatible with the tumorous change. However, final detailed histological examination revealed that the resected gland was histologically almost normal and had infiltration of scattered lymphocytes and clusters of lymphoid follicles with germinal centers, indicating a chronic autoimmune inflammation (Fig. 2). Unfortunately, remission was not obtained after the operation. Venous sampling of the neck and the chest for intact PTH was performed. The levels of intact PTH were higher near the superior vena cava than the other regions. From this result, reoperation was elected.

After obtaining the informed consent, on December 7, 2001, total thyroidectomy and paratracheal neck-upper thoracic dissection (Fig. 3) were performed. After the operation, plasma Ca decreased and intact PTH was not detected: below the assay threshold. At present this state continues up, and $1\alpha, 25\text{-(OH)}_2\text{D}_3$ and thyroxine are given for replacement. With regard to the histology of the parathyroid glands, examinations of 4 mm slices identified the two additional parathyroid glands, that is, 1.8×0.7 mm in the tissue around the thyroid gland and 5 mm diameter in the paratracheal region. The former was atrophic (Fig. 4), and the latter was normal without any tumorous change and histologically there was focal infiltration of lymphocytes. Immunohistochemical staining for PTH was weakly positive in approximately 5% of the cells within the parathyroid gland resected at the first operation but the intensity of staining was weaker than that generally observed for normal parathyroid glands. Other glands resected at the second operation had been completely sliced

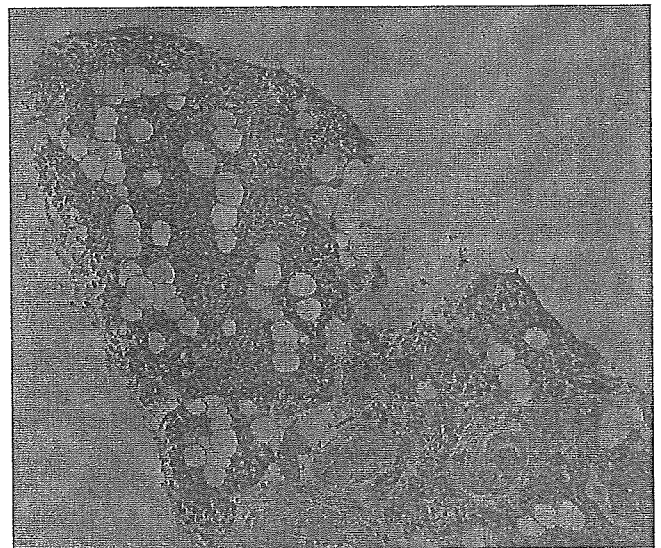


Figure 4. Pathology of the atrophic parathyroid gland resected at the second operation.

thin, and thus no block was available for staining.

Discussion

The patient had clinical manifestations featuring a drastic change from hypocalcemia to hypercalcemia with pathological findings of lymphoid follicles with germinal centers in

the parathyroid gland but no evidence of commonly observed parathyroid adenoma, hyperplasia or carcinoma. Spontaneous remission due to sudden hemorrhage or infarction of parathyroid adenomas was reported in several cases of primary hyperparathyroidism (2, 3). This can be confirmed by findings of degenerative or necrotic tissues with hemosiderin deposits. Such rare cases are considered to be different from our case since there was neither hemorrhagic nor infarctive trace in the present study.

The pathological findings observed seem to simply lead us to the conclusion that the complicated clinical course could be explained by a mechanism associated with chronic parathyroiditis similar to that of Hashimoto's disease. Hashimoto reported patients with diffuse goiter and clarified the four histological characteristics: diffuse lymphocytic infiltration, formation of lymphoid follicles, destruction of epithelial cells, and proliferation of fibrous tissue (4). The term "Hashimoto's disease" or "Hashimoto thyroiditis" is used to refer not only to goitrous thyroiditis but also chronic thyroiditis or autoimmune thyroiditis including atrophic and nongoitrous thyroiditis. Thyroid function of this disease is variable, from hypothyroidism or euthyroidism to hyperthyroidism. There are some case reports in which the clinical manifestations change as a result of transition between chronic thyroiditis and Graves' disease (5-16). Graves' disease is also classified among autoimmune organ-specific diseases characterized by lymphocytic infiltration of the thyroid and circulating antibodies directed to thyroid-stimulating hormone (TSH) receptors including thyroid-stimulating antibodies. Some patients with primary hypothyroidism subsequently develop hyperthyroidism (5-13). Several factors are considered to explain the changes of thyroid function: disappearance or decrease in titer of a blocking type of TSH receptor antibodies (7-9, 11-13) and emergence or increase in titer of a stimulating-type of TSH receptor antibodies (6-10, 12, 13). Although antibodies against the parathyroid gland were not studied in this case, there was the possibility that such parathyroid-stimulating and/or -blocking antibodies might be involved. Immunohistochemical staining for PTH was weakly positive in lymphoid follicles in the parathyroid gland of this case. However the results of immunohistochemical staining for PTH do not reveal the state of function of the parathyroid glands, whether they are hypofunctional or hyperfunctional. Negative or weak staining is caused by hormone deficiency or by hypersecretion. For example, the vasopressin content in the posterior lobe can be evaluated using magnetic resonance (MR) imaging. On MR T1-weighted images, the posterior lobe is demonstrated as a characteristic hyperintense signal under normal conditions (17), and the signal intensity of the posterior lobe is thought to reflect the content of neurosecretory granules containing vasopressin. The hyperintense signal of the posterior lobe of the pituitary gland is absent in diabetes insipidus on MR T1-weighted imaging, in which vasopressin-deficient hyposecretion occurs. In contrast, the vasopressin content in the posterior lobe is also decreased in patients with uncontrolled

diabetes mellitus, which was thought to be caused by persistent vasopressin hypersecretion (18).

Chronic parathyroiditis is rarely studied. In two extensive studies of parathyroid glands from 800 autopsies, only a single case of chronic parathyroiditis was found (19, 20). Hyperplastic parathyroiditis was also reported in a necropsy case, the function of which was unknown (21). Chronic parathyroiditis was also observed in a few cases of hypoparathyroidism (22, 23).

Thus far five cases of isolated hyperplastic parathyroiditis presenting with hyperparathyroidism have been reported. Two cases of chronic parathyroiditis associated with parathyroid hyperplasia and hyperparathyroidism are described by Bondeson et al (1). One case was a 62-year-old male whose serum calcium continually increased to 11.2 mg/dl (normal range 8.8-10.4 mg/dl). The patient became normocalcemic the day after parathyroidectomy, and serum calcium remained normal at follow-up after 4 years. The removed parathyroid glands contained lymphoid follicles with germinal centers. At the operation four enlarged parathyroid glands were identified. The three larger parathyroid glands were removed while the smallest one was left intact. The other case was a 53-year-old male whose serum calcium was increased to 10.8 mg/dl. Three enlarged parathyroid glands were removed while the smallest one, considered to be normal-sized, was left intact. This patient also became normocalcemic the day after the operation, and serum calcium remained normal at follow-up after 3 years. A third case of hyperparathyroidism associated with parathyroiditis coexisting with brachial-cleft cysts was reported (24). A 57-year-old man, whose calcium levels ranged from 13.52 to 13.60 mg/dl (normal range, 8.4-9.6 mg/dl) and whose PTH was 79.0 pg/ml (normal range, 0-55 pg/ml), had both enlarged inferior parathyroid glands removed. Both glands had similar features, including lymphoid tissue organized into follicles (some of which were replete with germinal centers), and numerous plasma cells (24). The fourth case of hyperparathyroidism associated with chronic parathyroiditis occurred in a multiple endocrine neoplasia type 1 (MEN-1) patient (25), and the fifth case remained hypercalcemic after removal of one parathyroid gland with lymphoid infiltration with germinal centers and one gland normal in microscopic appearance; the other glands were not investigated. In this case PTH was elevated to 164 pg/ml (normal range 10 to 55). Six months postoperatively serum calcium was 11.76 mg/dl and PTH was 90 pg/ml (26). All five cases presented clinically as primary hyperparathyroidism. The clinical course of our case is considered to have initially started as hypofunction, as in Hashimoto's disease, then to gradually have changed to hyperfunction as in Graves' disease, similar to autoimmune abnormalities often observed in the thyroid gland (5-13). Further similar case reports are required to analyze the details of the pathogenic mechanism of the parathyroid dysfunction associated chronic parathyroiditis.

In conclusion, we reported a case of hyperparathyroidism which initially presented with hypocalcemia associated with

lymphoid follicles with germinal centers in one parathyroid gland and later one atrophic and one normal parathyroid gland pathologically.

References

- 1) Bondeson AG, Bondeson L, Ljungberg O. Chronic parathyroiditis associated with parathyroid hyperplasia and hyperparathyroidism. *Am J Surg Pathol* 8: 211–215, 1984.
- 2) Kovacs KA, Gay JD. Remission of primary hyperparathyroidism due to spontaneous infarction of a parathyroid adenoma: Case report and review of the literature. *Medicine (Baltimore)* 77: 398–402, 1998.
- 3) Natsui K, Tanaka K, Suda M, Yasoda A, Yonemitsu S, Nakao K. Spontaneous remission of primary hyperparathyroidism due to hemorrhagic infarction in the parathyroid adenoma. *Intern Med* 35: 646–649, 1996.
- 4) Hashimoto H. Zur Kenntniss der lymphomatösen Veränderung der Schilddrüse (Struma lymphomatosa). *Arch Klin Chir* 97: 219–248, 1912 (in German).
- 5) Yamasaki H, Takeda K, Nakauchi Y, Suehiro T, Hashimoto K. Hypothyroidism preceding hyperthyroidism in patient with continuously positive stimulating antibody. *Internal Medicine* 34 (4): 247–250, 1995.
- 6) Kasagi K, Konishi J, Iida Y, Mori T, Torizuka K. Changes in thyroid-stimulating and TSH binding inhibitory activities in a patient who developed hyperthyroidism due to Graves' disease following primary hypothyroidism. *Clin Endocrinol* 25: 519–525, 1986.
- 7) Takeda K, Takamatsu J, Kasagi K, et al. Development of hyperthyroidism following primary hypothyroidism following primary hypothyroidism: a case report with changes in thyroid-related autoantibodies. *Clin Endocrinol* 28: 341–344, 1988.
- 8) Cho BY, Skong YK, Lee HK, Koh CS, Min HK. Graves' hyperthyroidism following primary hypothyroidism: sequential changes in various activities of thyrotropin receptor antibodies following primary hypothyroidism. *Acta Endocrinol (Copenh.)* 120: 447–450, 1989.
- 9) Takasu N, Yamada T, Sato A, et al. Graves' disease following hypothyroidism due to Hashimoto's disease: Studies of eight cases. *Clin Endocrinol (Oxf.)* 33: 687–698, 1990.
- 10) Tamai H, Kasagi K, Mizuno O, et al. Thyroid-stimulating antibody and thyrotropin-binding inhibitory immunoglobulin activity in hypothyroid patients who subsequently developed thyrotoxicosis. *Acta Endocrinol* 122: 499–504, 1990.
- 11) Kraiem Z, Baron E, Kahana L, Sadeh O, Sheinfeld M. Changes in stimulating and blocking TSH receptor antibodies in a patient undergoing three cycles of transition from hypo to hyperthyroidism and back to hypothyroidism. *Clin Endocrinol (Oxf.)* 36: 211–214, 1992.
- 12) Kasagi K, Hidaka A, Endo K, et al. Fluctuating thyroid function depending on the balance between stimulating and blocking types of TSH receptor antibodies: a case report. *Thyroid* 3: 315–318, 1993.
- 13) Miyauchi A, Amino N, Tamaki H, Kuma H. Coexistence of thyroid-stimulating and thyroid-blocking antibodies in a patient with Graves' disease who had transient hypothyroidism. *Am J Med* 85: 418–420, 1998.
- 14) Tamaki H, Amino N, Aozasa M, Mori M, Tanizawa O, Miyai K. Serial changes in thyroid-stimulating antibody and thyrotropin binding inhibitory immunoglobulins at the time of postpartum occurrence of thyrotoxicosis in Graves' disease. *J Clin Endocrinol Metab* 65: 324–330, 1987.
- 15) Kasagi K, Tamai H, Morita T, et al. Role of thyrotropin receptor antibodies in the development of hyperthyroidism: follow-up studies on nine patients with Graves' disease. *J Clin Endocrinol Metab* 68: 1189–1194, 1989.
- 16) Tamai H, Kasagi K, Morita T, et al. Thyroid response, especially to thyrotropin-binding inhibitory immunoglobulins, in euthyroid relatives of patients with Graves' disease: a clinical follow-up. *J Clin Endocrinol Metab* 71: 210–215, 1990.
- 17) Fujisawa I. Magnetic resonance imaging of the hypothalamic-neurohypophyseal system. *J Neuroendocrinol* 16: 297–302, 2004.
- 18) Fujisawa I, Murakami N, Furuto-Kato S, Araki N, Konishi J. Plasma and neurohypophyseal content of vasopressin in diabetes mellitus. *J Clin Endocrinol Metab* 81: 2805–2809, 1996.
- 19) Seemann N. Untersuchungen zur häufigkeit der lymphozytären parathyreiditis. *Dtsch Med Wochenschr* 92: 106–108, 1967 (in German).
- 20) Thiele J, Ries P, Georgii A. Spezielle und funktionelle pathomorphologie der epitelkörperchen in einem unausgewählten obduktionsgut (589 sektionen). *Virchows Arch A Pathol Anat Histol* 367: 195–208, 1975 (in German).
- 21) Boyce BF, Doherty VR, Mortimer G. Hyperplastic parathyroiditis a new autoimmune disease? *J Clin Pathol* 35: 812–814, 1982.
- 22) Kossling FK, Emmrich P. Demonstration eines falles von kindlichem morbus Addison mit hypoparathyreoidismus. *Verh Dtsch Ges Pathol* 55: 155–160, 1971 (in German).
- 23) Van de Casseye M, Gepts W. Case report: Primary (autoimmune?) parathyroiditis. *Virchows Arch A Pathol Anat* 361: 257–261, 1973.
- 24) Chetty R, Forder MD. Parathyroiditis associated with hyperparathyroidism and branchial cysts. *Am J Clin Pathol* 96: 348–350, 1991.
- 25) Sinha SN, McArdle JP, Shepherd JJ. Hyperparathyroidism with chronic parathyroiditis in a multiple endocrine neoplasia patient. *Aust NZ J Surg* 63: 981–982, 1993.
- 26) Vaizey CJ, Ali M, Gilbert JM. Chronic parathyroiditis associated with primary hyperplastic hyperparathyroidism. *J R Soc Med* 90: 336–337, 1997.

Analysis of Rat Insulin II Promoter-Ghrelin Transgenic Mice and Rat Glucagon Promoter-Ghrelin Transgenic Mice*

Received for publication, October 5, 2004, and in revised form, February 3, 2005
Published, JBC Papers in Press, February 8, 2005, DOI 10.1074/jbc.M411358200

Hiroshi Iwakura‡, Kiminori Hosoda‡§, Choel Son‡, Junji Fujikura‡, Tsutomu Tomita‡, Michio Noguchi‡, Hiroyuki Ariyasu‡, Kazuhiko Takaya‡¶, Hiroaki Masuzaki‡, Yoshihiro Ogawa‡, Tatsuya Hayashi‡, Gen Inoue‡, Takashi Akamizu||, Hiroshi Hosoda||**, Masayasu Kojima‡‡, Hiroshi Itoh‡, Shinya Toyokuni¶, Kenji Kangawa||**, and Kazuwa Nakao‡

From the ‡Department of Medicine and Clinical Science, Endocrinology and Metabolism and ¶Department of Pathology and Biology of Diseases, Kyoto University Graduate School of Medicine, 54 Shogoin Kawahara-cho, Sakyo-ku, Kyoto 606-8507, the ||Translational Research Center, Kyoto University Hospital, Kyoto 606-8507, the ‡‡Department of Molecular Genetics, Institute of Life Science, Kurume University, Fukuoka 839-0861, and the **Department of Biochemistry, National Cardiovascular Center Research Institute, Osaka 565-8565, Japan

We developed and analyzed two types of transgenic mice: rat insulin II promoter-ghrelin transgenic (RIP-G Tg) and rat glucagon promoter-ghrelin transgenic mice (RGP-G Tg). The pancreatic tissue ghrelin concentration measured by C-terminal radioimmunoassay (RIA) and plasma desacyl ghrelin concentration of RIP-G Tg were about 1000 and 3.4 times higher than those of nontransgenic littermates, respectively. The pancreatic tissue *n*-octanoylated ghrelin concentration measured by N-terminal RIA and plasma *n*-octanoylated ghrelin concentration of RIP-G Tg were not distinguishable from those of nontransgenic littermates. RIP-G Tg showed suppression of glucose-stimulated insulin secretion. Arginine-stimulated insulin secretion, pancreatic insulin mRNA and peptide levels, β cell mass, islet architecture, and GLUT2 and PDX-1 immunoreactivity in RIP-G Tg pancreas were not significantly different from those of nontransgenic littermates. Islet batch incubation study did not show suppression of insulin secretion of RIP-G Tg *in vitro*. The insulin tolerance test showed lower tendency of blood glucose levels in RIP-G Tg. Taking lower tendency of triglyceride level of RIP-G Tg into consideration, these results may indicate that the suppression of insulin secretion is likely due to the effect of desacyl ghrelin on insulin sensitivity. RGP-G Tg, in which the pancreatic tissue ghrelin concentration measured by C-RIA was about 50 times higher than that of nontransgenic littermates, showed no significant changes in insulin secretion, glucose metabolism, islet mass, and islet architecture. The present study raises the possibility that desacyl ghrelin may have influence on glucose metabolism.

Ghrelin is a 28-amino acid peptide with unique modification of acylation, which is essential for its biological action (1). Ghrelin was originally identified in rat stomach as an endogenous ligand for an orphan receptor, which has been so far called

growth hormone secretagogue receptor (GHS-R)¹ (1). Ghrelin expression is detected in the stomach, intestine, hypothalamus, pituitary gland, kidney, placenta, and testis (2–6). Ghrelin is involved in a wide variety of the functions, including the regulation of growth hormone release, food intake, gastric acid secretion, gastric motility, blood pressure, and cardiac output (7–19).

Recently Date *et al.* (20) reported that ghrelin is present in α cells of normal human and rat pancreatic islets. Volante *et al.* (21) described ghrelin-expression in β cells of human islet. Wierup *et al.* and Prado *et al.* reported that ghrelin-expressing cells are a new islet cell type distinct from α , β , δ , and PP cells in human, rat, and mouse islets (22–24). Although there was no apparent change of plasma insulin levels in ghrelin null mouse (25, 26), which may indicate that ghrelin is not a direct regulator of insulin secretion in the physiological condition, there have been several reports of the effect of pharmacological dose of ghrelin on insulin secretion. Broglio *et al.*, Egido *et al.*, and Reimer *et al.* have reported that ghrelin has an inhibitory effect on insulin secretion (27–30). Adeghate *et al.*, Date *et al.*, and Lee *et al.* have reported that ghrelin stimulates insulin secretion (20, 31, 32). Salehi *et al.* have reported ghrelin has both inhibitory and stimulatory effects depending on its concentration (33). Therefore, there is still a lot of controversy about the localization of ghrelin in the pancreas and the effects of ghrelin on the insulin secretion. As for the effects of desacyl ghrelin on insulin secretion, Broglio *et al.* (34) have reported that acute desacyl ghrelin administration has no effect on insulin secretion in human but that it counteracts the inhibitory effect of *n*-octanoylated ghrelin on insulin secretion when co-administered with *n*-octanoylated ghrelin (35).

Here we developed and analyzed two types of transgenic mice: rat insulin II promoter-ghrelin transgenic mice (RIP-G Tg) and rat glucagon promoter-ghrelin transgenic mice (RGP-G Tg). The purpose of this study was to clarify the effect of transgenic overexpression of ghrelin cDNA in pancreatic islets.

EXPERIMENTAL PROCEDURES

Generating RIP- and RGP-ghrelin Transgenic Mice—Mouse stomach cDNA library was constructed from 1 μ g of mouse stomach poly(A)⁺

* This work was supported by research grants from the Japanese Ministry of Education, Culture, Sports, Science and Technology, the Japanese Ministry of Health, Labor and Welfare. The costs of publication of this article were defrayed in part by the payment of page charges. This article must therefore be hereby marked "advertisement" in accordance with 18 U.S.C. Section 1734 solely to indicate this fact.

§ To whom correspondence should be addressed. Tel.: 81-75-751-3172; Fax: 81-75-771-9452; E-mail: kh@kuhp.kyoto-u.ac.jp.

RNA with a cDNA synthesis kit (Amersham Biosciences). Mouse ghrelin cDNA was isolated from this library, using rat ghrelin cDNA as a probe. A fusion gene comprising RIP and mouse ghrelin cDNA coding sequences was designed. The purified fragment (10 µg/ml) was microinjected into the pronucleus of fertilized C57/B6J mice (SLC, Shizuoka, Japan) eggs. The viable eggs were transferred into the oviducts of pseudopregnant female ICR mice (SLC) using standard techniques. Transgenic founder mice were identified by Southern blot analysis of tail DNAs using the mouse ghrelin cDNA fragment as a probe. RGP-G Tg was generated similarly. Transgenic mice were used as heterozygotes. Animals were maintained on standard rat food (CE-2, 352 kcal/100 g, Japan CLEA, Tokyo, Japan) on a 12-h light/12-h dark cycle. All experimental procedures were approved by the Kyoto University Graduate School of Medicine Committee on Animal Research.

Immunohistochemistry—Formalin-fixed, paraffin-embedded tissue sections were immunostained using the avidin-biotin peroxidase complex method (Vectastain "ABC" Elite kit, Vector Laboratories, Burlingame, CA) as described previously (36). Serial sections were used, and the thickness of each section was 5 µm. Sections were incubated with anti-C-terminal ghrelin [13–28] (1:1000 at final dilution), anti-N-terminal ghrelin [1–11] (1:2000) (1), which recognizes the *n*-octanoylated portion of ghrelin, anti-glucagon (1:500), anti-insulin (1:500), anti-somatostatin (1:500), anti-pancreatic polypeptide (PP, 1:500, DAKO, Glostrup, Denmark), anti-PDX-1 (1:2000, kindly provided by Christopher V. E. Wright) (37), and anti-GLUT2 (1:200, kindly provided by Bernard Thorens) (38) antisera. Quantification of β cell area was performed in insulin-stained sections by using Axio Vision (Carl Zeiss, Hallbergmoos, Germany) and Scion Image (Scion Corp., Frederick, MD). Ten sections (200-µm interval) for each mouse (*n* = 5) were analyzed. The percentage of β cell area in the pancreas was determined by dividing the area of all insulin-positive cells in one section by the total area of the section.

Measurements of Plasma and Tissue Ghrelin Concentrations—Plasma was sampled from 10-week-old RIP-G Tg and their nontransgenic littermates under ad libitum feeding states considering the promoter activity. From RGP-G Tg and their littermates, it was sampled after overnight fast. Blood was withdrawn from the retroorbital vein or the proximal end of the portal vein under ether anesthesia, immediately transferred to chilled siliconized glass tubes containing Na₂EDTA (1 mg/ml) and aprotinin (1000 KIU/ml, Ohkura Pharmaceutical, Kyoto, Japan), and centrifuged at 4 °C. Hydrogen chloride was added to the samples at a final concentration of 0.1 N immediately after separation of plasma. Plasma was immediately frozen and stored at -80 °C until assay. Plasma ghrelin concentration was determined by desacyl ghrelin enzyme-linked immunosorbent assay kit and active-ghrelin enzyme-linked immunosorbent assay kit that recognizes *n*-octanoylated ghrelin (Mitsubishi Kagaku Iatron, Tokyo, Japan).

As for measurement of tissue ghrelin concentration, pancreata or stomachs were taken from the 8-week-old male mice. The rumen was removed from the stomach. Samples were diced and boiled for 5 min in the 10-fold v/w of water. Acetic acid was added to each solution so that the final concentration was adjusted to 1 M, and the tissues were homogenized. The supernatants were obtained after centrifugation. Tissue ghrelin concentration was determined by radioimmunoassay (RIA) using anti-ghrelin [13–28] antiserum (C-RIA) and anti-ghrelin [1–11] antiserum (N-RIA) as described previously (39).

Measurements of Body Weight and Food Consumption—Mice were housed individually and were allowed free access to standard rat chow. Body weights of mice were measured weekly. Daily food intake was measured by weighing the pellets between 9:00 and 10:00 a.m.

Measurements of % Body Fat and Visceral/Subcutaneous Fat Mass Ratio—Forty-week-old mice were anesthetized with pentobarbital. Percent body fat and visceral/subcutaneous fat mass ratio of mice were measured by Latheta LTC-100 (ALOKA, Tokyo, Japan).

Glucose and Insulin Tolerance Tests—For the glucose tolerance test, after overnight fast, the mice were injected with 1.5 g/kg glucose intraperitoneally. For the insulin tolerance test, after a 4-h fast, mice were injected with 2.0 milliuunits/g human regular insulin (Novolin R; Novo Nordisk, Bagsvaerd, Denmark) intraperitoneally. Blood was sampled from the tail vein before and 15, 30, 60, 90, and 120 min after the injection. Blood glucose levels were determined by glucose oxidase method using Glutest sensor (Sanwa Kagaku, Kyoto, Japan).

Insulin Release—After overnight fast, the mice were injected with 3.0 g/kg glucose or 0.25 g/kg L-arginine intraperitoneally. Plasma was sampled from the tail vein before and 2, 5, 15, 30, and 60 min after the injection using heparin coated tubes. The measurement of insulin concentration was carried out by enzyme-linked immunosorbent assay using ultra-sensitive rat insulin kit (Morinaga, Yokohama, Japan).

Pancreatic Insulin Concentration—As for measurement of pancreatic

insulin concentration, pancreata were obtained from the mice under the ether anesthesia and homogenized in acid-ethanol. The supernatants were used for assay after centrifugation.

Batch Incubation of Islet—Under the pentobarbital anesthesia, Type IV collagenase (Worthington, Lakewood, NJ) dissolved in Hanks' balanced salt solution (1.5 mg/ml) was injected into mouse pancreatic duct. Pancreas was removed and incubated at 37 °C for 14 min. After washing out collagenase by Hanks' balanced salt solution, islets were collected by Ficoll gradient and manually picked up so that the sizes of the islets were equal. Islets were incubated at 37 °C in RPMI1640 containing 10% fetal calf serum for 2 h and then in Krebs-Ringer bicarbonate buffer containing 3.3 mM glucose and 0.2% bovine serum albumin for 30 min. Five islets were incubated at 37 °C in 500 µl of Krebs-Ringer bicarbonate buffer containing 0.2% bovine serum albumin and 3.3 or 8.7 or 16.7 mM glucose for 1 h. After centrifugation, the supernatants were collected. Insulin concentrations in supernatants were determined by rat insulin kit (Morinaga, Yokohama, Japan).

Northern Blot Analysis and Real-time Quantitative RT-PCR—Total RNA was extracted from pancreata using RNeasy mini kit (Qiagen K.K., Tokyo, Japan). Filters containing 5 µg of total RNA were prepared. Northern blot analyses were performed as described previously (36) using the mouse insulin II cDNA and human β-actin cDNA (Clontech, Palo Alto, CA) as probes. To confirm that approximately equal amounts of total RNA were assayed in Northern blot hybridization analysis, the density of 18 S rRNA in the gel and signal of β-actin in each lane was used. The hybridization signal intensity was quantitated using an image analyzer BAS-2500 (Fuji Photo Film, Tokyo, Japan). Reverse transcription (RT) was performed with random hexamer and SuperScript II reverse transcriptase (Invitrogen). Real-time quantitative PCR was performed with ABI PRISM 7700 Sequence Detection System (Applied Biosystems, Foster City, CA). The following primers and TaqMan probes were used: mouse GHS-R (sense, 5'-CACCAACCTCT-ACCTATCCAGCAT-3'; antisense, 5'-CTGACAAACTGGAAGAGTTTG-CA-3'; TaqMan probe, 5'-TCCGATCTGCTCATCTTCCTGTGCATG-3'); mouse ghrelin (sense, 5'-GCATGCTCTGGATGGACATG-3'; antisense, 5'-TGGTGGCTTCTTGGATTCCT-3'; TaqMan probe, 5'-AGCCAGAGCCAGAAAGCCCA-3').

Lipid Measurements—Blood was collected from the retroorbital vein of 35-week-old RIP-G Tg and their nontransgenic littermates. After separation of serum, total cholesterol, triglyceride, free fatty acid, and HDL-cholesterol levels in serum were determined by Cholesterol E-test Wako, Triglyceride E-test Wako, NEFA C-test Wako, and HDL-cholesterol E-test Wako (Wako Pure Chemical Industries, Osaka, Japan).

Statistical Analysis—All values were expressed as means ± S.E. Statistical significance of difference in mean values was assessed by repeated measures analysis of variance or Student's *t* test.

RESULTS

Distribution of Ghrelin in Normal Mouse Pancreas—We first examined which cell type of islet cells expresses ghrelin in mouse by immunohistochemistry using anti-C-terminal ghrelin antiserum. In the most of the islets no ghrelin-like immunoreactivity was detected. C-terminal ghrelin-like immunoreactivity was observed in the periphery of minor proportion of islets of wild type mice (Fig. 1A). Most of the ghrelin-positive cells were also glucagon-positive by serial section analysis (Fig. 1B), whereas most of the glucagon-positive cells were not ghrelin-positive.

Generation of RIP- and RGP-ghrelin Transgenic Mice—A fusion gene comprising RIP and mouse ghrelin cDNA coding sequences was designed so that ghrelin expression might be targeted to the pancreatic β cells (Fig. 2A). The ghrelin mRNA level of RIP-G Tg in pancreas determined by quantitative RT-PCR was about 215 times higher than that of nontransgenic littermates (215.3 ± 40.6 versus 1.0 ± 0.025 arbitrary units, *n* = 5, *p* < 0.01). There was also an increase in ghrelin mRNA levels in brain of RIP-G Tg (242.6 ± 17.6 versus 89.1 ± 27.3 arbitrary unit, *n* = 5, *p* < 0.01). To confirm the expression of ghrelin transgene in pancreatic β cells, we performed an immunohistochemical analysis using anti-C-terminal ghrelin antiserum. C-terminal ghrelin-like immunoreactivity was observed in the nearly whole area of the islets of the RIP-G Tg (Fig. 2C), whereas it was only seen in the periphery of the islets

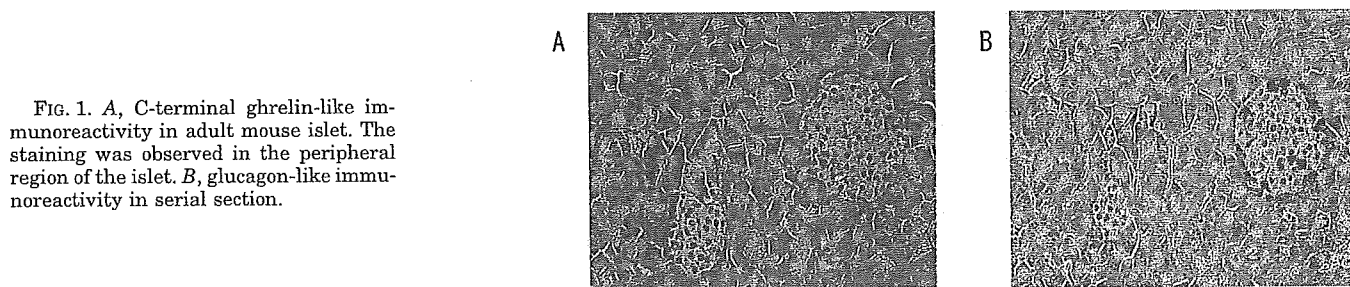


FIG. 1. A, C-terminal ghrelin-like immunoreactivity in adult mouse islet. The staining was observed in the peripheral region of the islet. B, glucagon-like immunoreactivity in serial section.

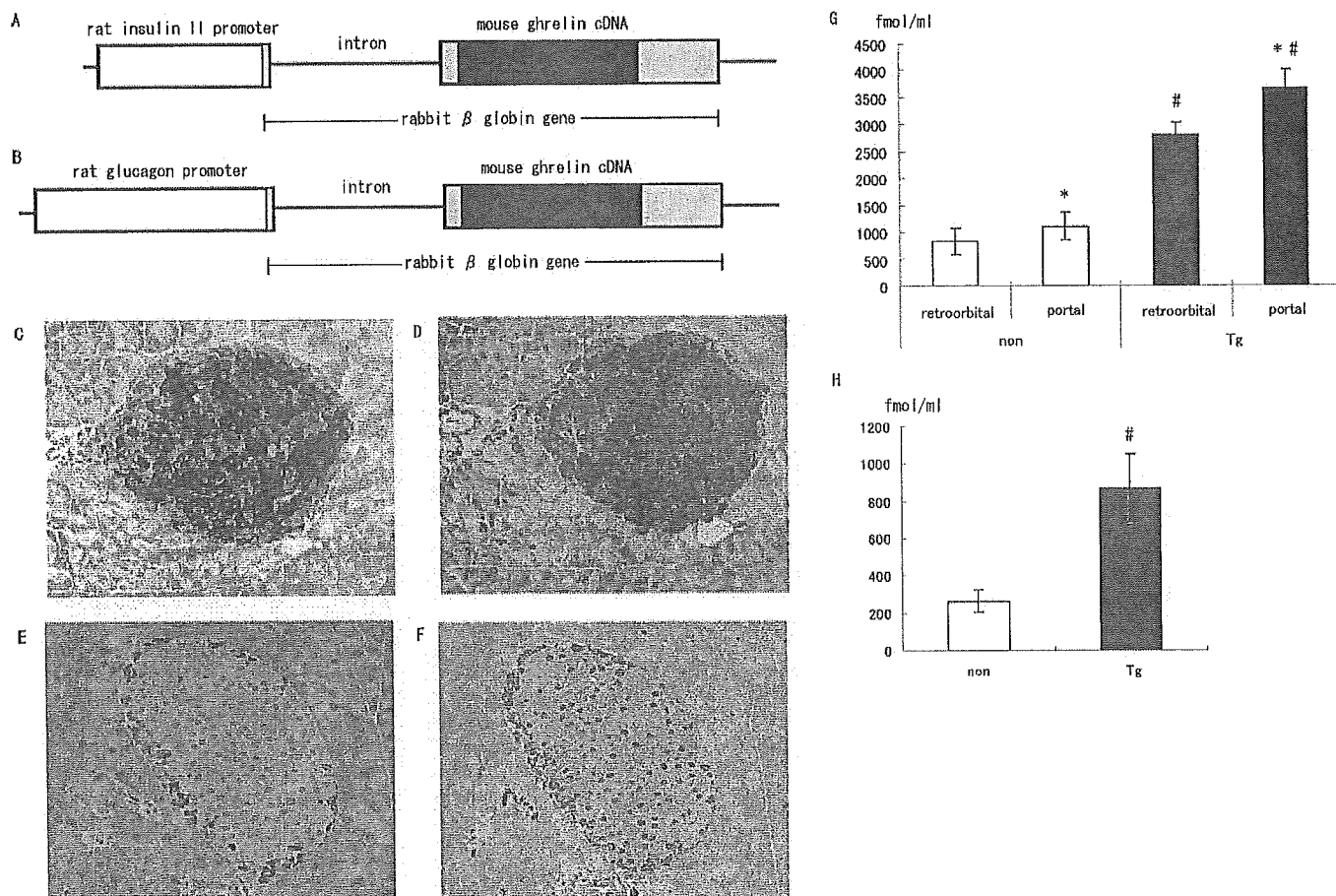


FIG. 2. A, structure of RIP-ghrelin transgene. B, structure of RGP-ghrelin transgene. C and D, pancreatic islet of RIP-ghrelin transgenic mouse stained with anti-C-terminal ghrelin (C) and anti-N-terminal ghrelin antisera (D). E and F, pancreatic islet of RGP-ghrelin transgenic mouse stained with anti-C-terminal ghrelin (E) and anti-N-terminal ghrelin antisera (F). G, plasma ghrelin levels collected from retroorbital and portal veins in RIP-G Tg. *, $p < 0.05$ compared with retroorbital vein. #, $p < 0.01$ compared with nontransgenic littermates. H, the step-up of ghrelin concentration from retroorbital vein to portal vein in RIP-G Tg. #, $p < 0.01$ compared with their nontransgenic littermates.

of their nontransgenic littermates (Fig. 1A). Immunohistochemical analysis using anti-N-terminal ghrelin antiserum showed the same staining pattern (Fig. 2D), indicating that *n*-octanoylated ghrelin may be produced in β cells of this transgenic mouse. We also stained the brain section of RIP-G Tg. No ghrelin-like immunoreactivity was detected either with anti-C-terminal or anti-N-terminal ghrelin antisera (data not shown). The pancreatic tissue ghrelin concentration of RIP-G Tg measured by C-RIA was about 1000 times higher than that of their nontransgenic littermates (1024 ± 108.9 fmol/mg versus 1.2 ± 0.1 fmol/mg, $n = 5$, $p < 0.01$). This concentration was about one third of the nontransgenic stomach concentration (3558.1 ± 51.0 fmol/mg, $n = 5$). The pancreatic tissue ghrelin concentration of RIP-G Tg measured by N-RIA tended to be also higher than that of their nontransgenic littermates (0.054 ± 0.017 fmol/mg versus 0.038 ± 0.006 fmol/mg, $n = 5$, NS; not significant), but it did not reach statistical significance. Plasma desacyl ghrelin concentration of RIP-G Tg was about 3.4 times

higher than that of nontransgenic littermates under the ad libitum feeding states (2805.5 ± 236.4 versus 825.9 ± 244.4 fmol/ml, $n = 5$, $p < 0.01$, Fig. 2G). We also measured desacyl ghrelin levels in portal vein of the mice. In the nontransgenic mice, the portal desacyl ghrelin level was significantly higher than that in retroorbital vein (1108.0 ± 257.3 fmol/ml versus 825.9 ± 244.4 fmol/ml, $n = 5$, $p < 0.05$, Fig. 2G). The desacyl ghrelin concentration collected from portal vein of RIP-G Tg at the same time was much higher than that of nontransgenic littermates (3671.8 ± 328.6 versus 1108.0 ± 257.3 fmol/ml, $n = 5$, $p < 0.01$, Fig. 2G). The step-up of desacyl ghrelin concentration from retroorbital vein to portal vein of RIP-G Tg was significantly higher than that of nontransgenic littermates (866.3 ± 182.2 fmol/ml versus 262.9 ± 59.8 fmol/ml, $p < 0.01$, Fig. 2H). Plasma *n*-octanoylated ghrelin levels in retroorbital and portal vein of RIP-G Tg tended to be higher than those of their nontransgenic littermates (retroorbital: 78.5 ± 13.4 versus 66.1 ± 7.1 fmol/ml, $n = 5$, NS; portal: 104.6 ± 15.3 versus

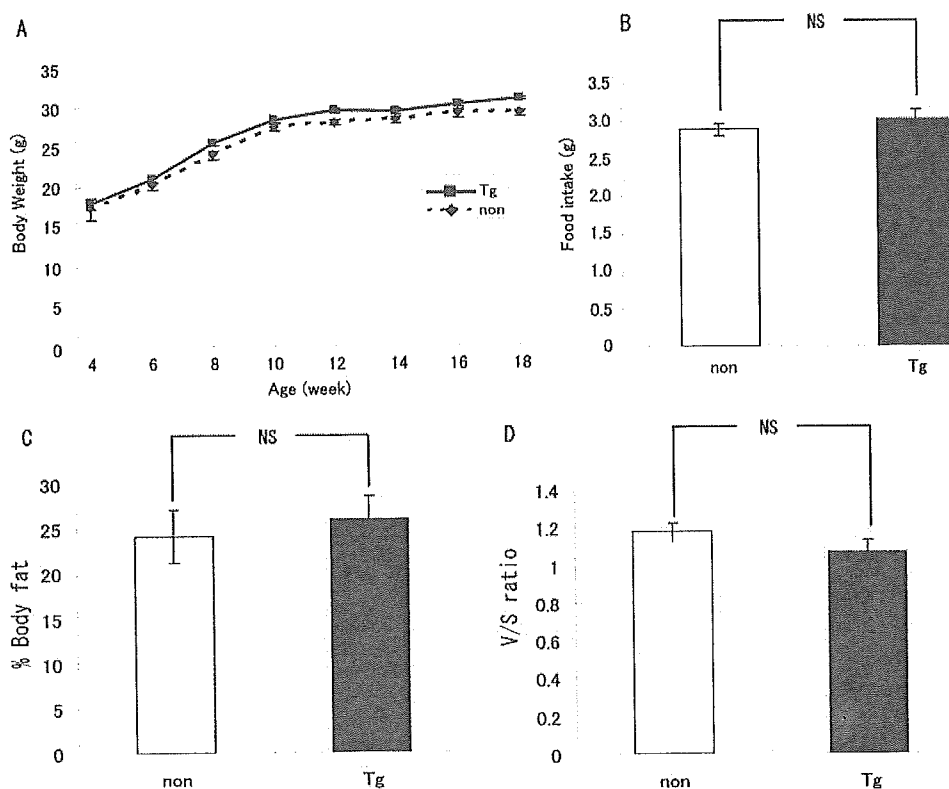


FIG. 3. A, body weight of RIP-G Tg (*Tg*) and their nontransgenic littermates (*non*). B, food intake of RIP-G Tg (*Tg*) and their nontransgenic littermates (*non*). Percent body fat (C) and visceral/subcutaneous fat ratio (D) of RIP-G Tg and their nontransgenic littermates (*non*).

71.4 ± 9.0 fmol/ml, $n = 5$, NS), but it did not reach statistical significance.

We also generated RGP-G Tg, in which ghrelin expression is targeted to the pancreatic α cells (Fig. 2B). The ghrelin mRNA level in pancreas of RGP-G determined by quantitative RT-PCR was about 16 times higher than that of nontransgenic littermates (16.3 ± 1.7 versus 1.0 ± 0.24 arbitrary unit, $n = 5$, $p < 0.01$). The ghrelin mRNA level in duodenum of RGP Tg was not statistically different from that of nontransgenic littermates (520.1 ± 111.1 versus 379.1 ± 37.6 arbitrary unit, $n = 5$, NS). The ghrelin mRNA level in brain of RGP Tg was not distinguishable from that of nontransgenic littermates (72.0 ± 6.4 versus 71.8 ± 7.8 arbitrary unit, $n = 5$, NS). Immunohistochemical analysis showed ghrelin-like immunoreactivity in the periphery of the pancreatic islet of RGP-ghrelin transgenic mouse by both anti-C-terminal ghrelin and anti-N-terminal ghrelin antisera (Fig. 2, E and F). The pancreatic tissue ghrelin concentrations of RGP-G Tg measured by C-RIA were about 50 times higher than those of their nontransgenic littermates (48.9 ± 2.5 fmol/mg versus 1.2 ± 0.1 fmol/mg, $n = 5$, $p < 0.01$). The pancreatic tissue ghrelin concentration of RGP-G Tg measured by N-RIA tended to be higher than that of their nontransgenic littermates (0.076 ± 0.019 fmol/mg versus 0.038 ± 0.006 fmol/mg, $n = 5$, NS), but it did not reach statistical significance. The plasma desacyl ghrelin concentrations in retroorbital vein were not elevated in RGP-G Tg after overnight fasting compared with nontransgenic littermates (661.6 ± 38.0 versus 1024.7 ± 27.1 fmol/ml, $n = 5$). The portal desacyl ghrelin concentrations of RGP-G Tg were also indistinguishable from those of their nontransgenic littermate (1320.6 ± 164.7 versus 1442.9 ± 361.5 fmol/ml, $n = 5$, NS). Plasma *n*-octanoylated ghrelin levels in retroorbital and portal vein of RGP-G Tg were indistinguishable from those of their nontransgenic littermates (retroorbital: 98.3 ± 18.7 versus 133.5 ± 25.3 fmol/ml, $n = 5$, NS; portal: 154.3 ± 20.7 versus 198.9 ± 34.9 fmol/ml, $n = 5$, NS).

Body Weight, Food Consumption, and Percent Body Fat—There was no significant difference in body weight and food intake between RIP-G Tg and their nontransgenic littermates (Fig. 3). Percent body fat and visceral/subcutaneous ratio of RIP-G Tg were not different from those of nontransgenic littermates (Fig. 2, C and D). No significant changes were observed in RGP-G Tg, either (data not shown).

Glucose Metabolism and Insulin Secretion—Although no significant differences in blood glucose levels were noted between RIP-G Tg and their nontransgenic littermates on the fasting state and intraperitoneal glucose tolerance tests (Fig. 4, A and C), plasma insulin levels 2 and 30 min after the glucose injection were significantly decreased in RIP-G Tg compared with those in their nontransgenic littermates (Fig. 4D). Suppression of insulin secretion was not observed in RIP-G Tg on intraperitoneal injection of arginine (Fig. 4G). Blood glucose level of RIP-G Tg in the insulin tolerance test tended to be lower than those of their nontransgenic littermates, but it did not reach statistical significance (Fig. 4H).

No significant differences in blood glucose or insulin levels were observed between RGP-G Tg and their nontransgenic littermates on the fasting state, ad libitum feeding, or intraperitoneal glucose or arginine injection (Fig. 4, B, E, and F, and data not shown). Blood glucose levels on insulin tolerance test showed no differences between RGP-ghrelin and their nontransgenic littermates (data not shown).

Islet Architecture and β Cell Mass—We studied the tissue sections of RIP-G Tg to explore the effect of ghrelin on the islet architecture and β cell mass. There were no obvious abnormalities in the intra islet cytoarchitecture and cell number of insulin, glucagon, somatostatin, and PP cells in the islets of the RIP-G Tg (Fig. 5A–D). The intensity of staining of these four islet hormones in the islets of the RIP-G Tg was not apparently different from those of nontransgenic littermates. The ratio of the β cell area to whole pancreas was not changed significantly

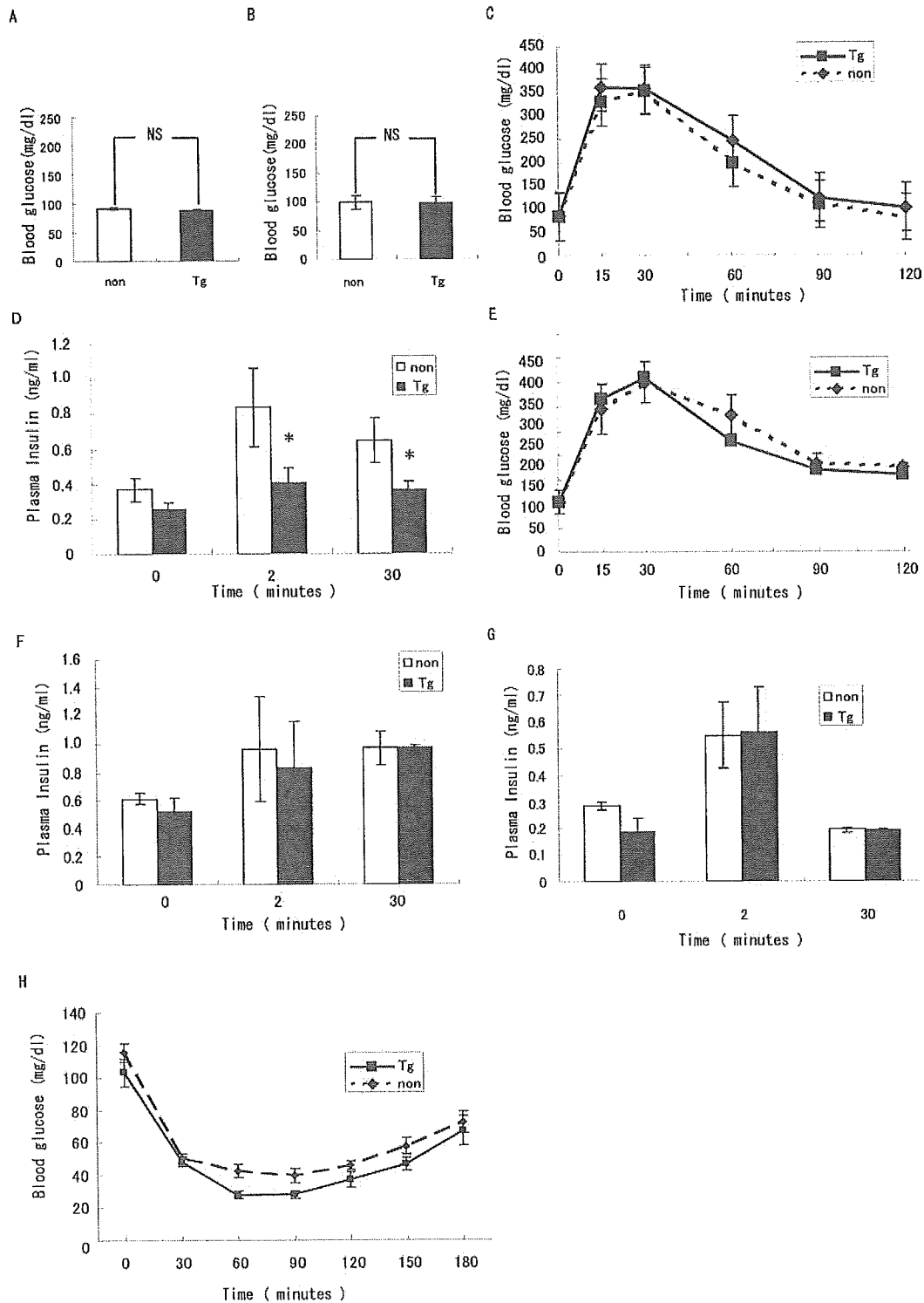


FIG. 4. *A* and *B*, blood glucose levels after overnight fast in RIP-G Tg (*A*) and RGP-G Tg (*B*) (*Tg*) and their nontransgenic littermates (*non*). *C* and *E*, intraperitoneal (IP) glucose tolerance test (1.5 g/kg) in RIP-G Tg (*C*) and RGP-G Tg (*E*) (*Tg*) and their nontransgenic littermates (*non*). *D* and *F*, plasma insulin concentration after intraperitoneal glucose (3g/kg) injection in RIP-G Tg (*D*) and RGP-G Tg (*F*) (*Tg*) and their nontransgenic littermates (*non*). *G*, plasma insulin concentration after intraperitoneal arginine (0.25g/kg) injection in RIP-G Tg (*Tg*) and their nontransgenic littermates (*non*). *H*, insulin (2.0 units/kg) tolerance test in RIP-G Tg (*Tg*) and their nontransgenic littermates (*non*). Values are represented as mean \pm S.E. *, $p < 0.05$ compared with nontransgenic littermates.

(Fig. 5I). We also studied the tissue sections of RGP-G Tg and found no significant differences (Fig. 5, *E-H*, and *J*).

Expression of Insulin mRNA and Insulin Content—Because RIP-G Tg showed suppression of insulin secretion, we examined pancreatic mRNA expression and peptide content of insulin in RIP-G Tg and their nontransgenic littermates by Northern blot analysis and RIA. The insulin mRNA in RIP-G Tg did

not differ from those of their nontransgenic littermates (Fig. 6, *A* and *B*). No significant differences of insulin contents were observed between RIP-G Tg and their nontransgenic littermates (Fig. 6C).

PDX-1 and GLUT2 Immunoreactivity—We examined the immunoreactivity of PDX-1 and GLUT2 in RIP-G Tg. The staining intensities of PDX-1 and GLUT2 in the RIP-G Tg (Fig. 7, *A*

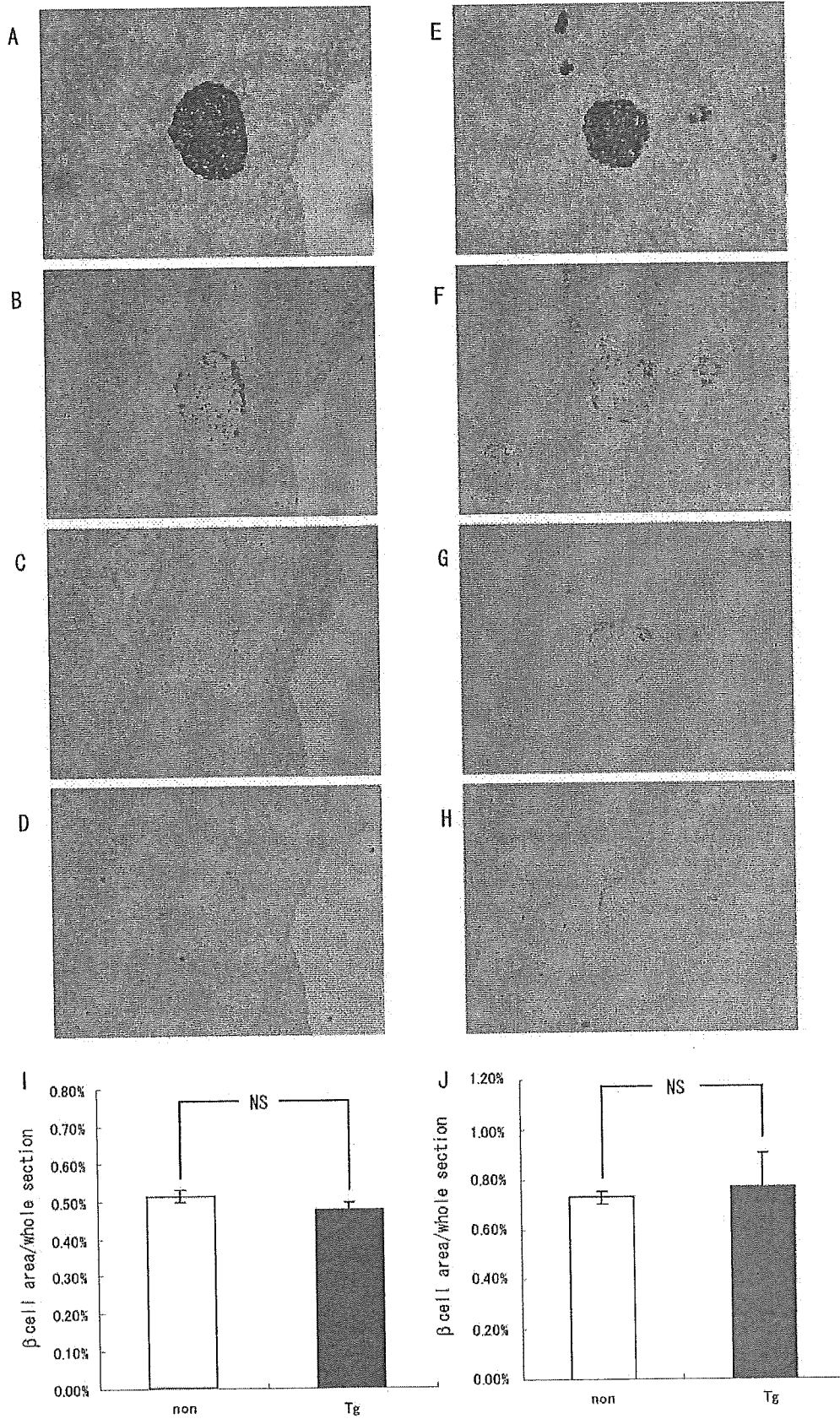


FIG. 5. Islet morphology and β cell area in RIP-G Tg (A-D) and RGP-G Tg (E-H). The sections were stained with anti-insulin (A and E), anti-glucagon (B and F), anti-somatostatin (C and G), and anti-PP antiserum (D and H). I and J, the ratio of β cell area to that of whole section in RIP-G Tg (I) and RGP-G Tg (J). non, nontransgenic littermates; Tg, RIP-G Tg; NS, not significant.

and C) were not apparently different from those in the non-transgenic littermates (Fig. 7, B and D).

Expression of GHS-R mRNA—To rule out possible down-

regulation of GHS-R due to chronic exposure to high level ghrelin, we measured the expression level of GHS-R mRNA in pancreas and pituitary by real-time quantitative RT-PCR.

FIG. 6. mRNA level and peptide content of insulin in RIP-G Tg (*Tg*) and their nontransgenic littermates (*non*) pancreas. A, representative blot of Northern blot analysis of insulin; B, insulin mRNA levels; C, insulin peptide contents. NS, not significant.

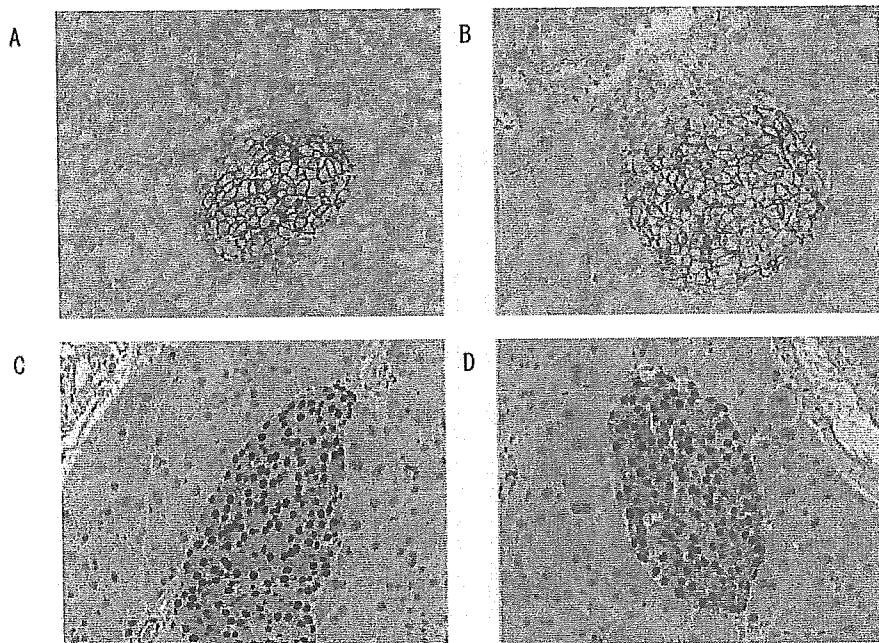
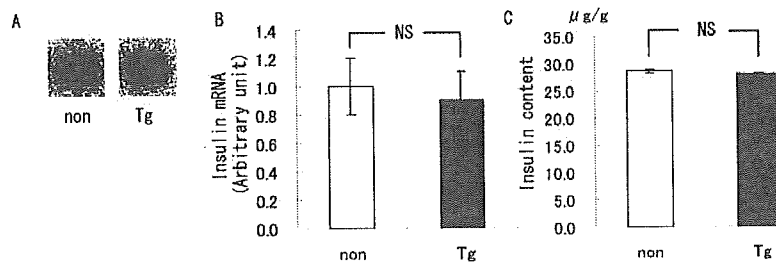


FIG. 7. A and B, immunoreactivity of Glut-2 in the islet of RIP-G Tg (A) and nontransgenic littermates (B). C and D, immunoreactivity of PDX-1 in the islet of RIP-G Tg (C) and nontransgenic littermates (D).

There were no significant differences in GHS-R mRNA levels between RIP-G Tg and their nontransgenic littermates either in pancreas (Fig. 8A) or in pituitary (Fig. 8B).

Batch Incubation of Islets—The insulin secretion from isolated islet of RIP-G Tg by batch incubation was indistinguishable from that of nontransgenic littermates, in 3.3 or 8.7 or 16.7 mM glucose conditions (Fig. 9).

Lipid Metabolism—Plasma total cholesterol level of RIP-G Tg tended to be lower than those of nontransgenic littermates, but it did not reach statistical significance (total cholesterol: 85.4 ± 6.9 versus 79.4 ± 7.5 mg/dl, $n = 6$, NS). The plasma triglyceride level of RIP-G Tg tended to be lower than that of nontransgenic littermates, but it did not reach statistical significance (154.5 ± 11.0 versus 136.9 ± 10.3 mg/dl, $n = 6$, NS). Free fatty acid level and HDL-cholesterol level of RIP-G Tg were not significantly different from those of nontransgenic littermates (free fatty acid; 0.44 ± 0.05 versus 0.48 ± 0.07 mEq/liter, $n = 6$, NS, HDL-cholesterol; 46.1 ± 2.3 versus 44.9 ± 3.4 mg/dl, $n = 6$, NS).

DISCUSSION

In wild-type mice, no ghrelin-like immunoreactivity was detected in most of the islets. C-terminal ghrelin-like immunoreactivity was observed in the periphery of minor proportion of islets of wild type mice, which is consistent with a previous report (24). By the serial section analysis, most of the ghrelin-producing cells also showed glucagon-like immunoreactivity. These findings indicate that ghrelin was expressed in minor proportion of mouse pancreatic α cells. Expression of ghrelin was not detected in pancreatic β cells of wild type mice.

In the present study we developed RIP-G Tg, in which pancreatic ghrelin concentration measured by C-RIA was ~ 1000 times higher than that of nontransgenic littermates. By immu-

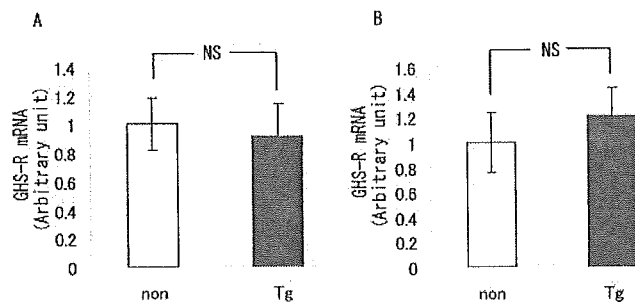


FIG. 8. mRNA level of GHS-R determined by quantitative RT-PCR in pancreas (A) and pituitary (B) of RIP-G Tg (*Tg*) and their nontransgenic littermates (*non*). NS, not significant.

nohistochemistry using anti-C-terminal ghrelin [13–28] antiserum we detected C-terminal ghrelin-like immunoreactivity in almost the whole area of islets. Therefore, because ghrelin was not detected in β cells of control mice by immunohistochemistry, ghrelin transgene driven by RIP was considered to be expressed in β cells.

We also found about 3 times higher expression level of ghrelin mRNA in the brain of RIP-G Tg compared with that of nontransgenic littermates, which could not be detected by immunohistochemistry. Although a small amount of ghrelin has been reported to be expressed in brain, which can be detected by immunohistochemistry only after colchicine treatment (1), there have been controversies as to whether this small amount of ghrelin in the brain has a biological role. Because the food intake of RIP-G Tg was not different from that of nontransgenic littermates, the ghrelin produced by transgene in the brain seems not to show bioactive effect of *n*-octanoylated ghrelin.

By immunohistochemistry using anti-ghrelin [1–11] anti-

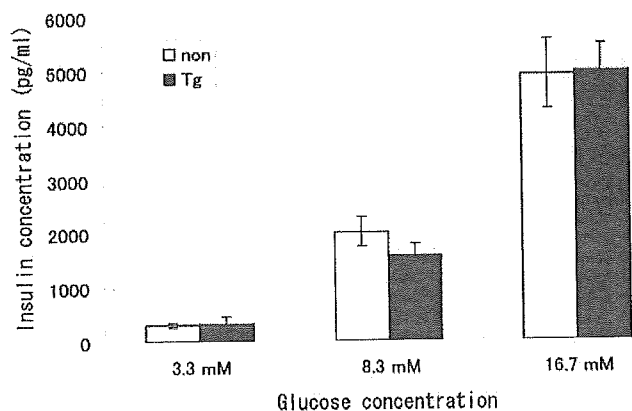


FIG. 9. Batch incubation study of isolated islets of RIP-G Tg (Tg) and their nontransgenic littermates (non).

serum that recognizes the *n*-octanoylated portion of ghrelin, ghrelin-like immunoreactivity was also demonstrated in nearly whole area of islets of RIP-G Tg, indicating the production of *n*-octanoylated ghrelin in β cells. This finding indicates that the mechanism of acylation may exist not only in pancreatic α cells but also in β cells. This is reasonable, because α and β cells are pancreatic endocrine cells derived from common precursor cells (40). Because the N-RIA/C-RIA ratio of the pancreatic tissue ghrelin concentration of RIP-G Tg was much lower than that of the stomach (0.0053% versus 11.67%, $p < 0.01$), the ability of acylation in β cell might be lower than that of in ghrelin-producing cell in the stomach (X/A-like cell). It is possible that exocrine pancreatic enzymes might interfere with the results, although these were inactivated by boiling before extraction. The other possibility is that because of the formalin fixation of ghrelin in the tissue section the epitope recognized by immunohistochemistry using anti-ghrelin [1–11] antiserum might not be exactly the same as that recognized by N-RIA or enzyme-linked immunosorbent assay. Because the amount of *n*-octanoylated ghrelin was so little that it could not be detected by RIA if any, we considered that the phenotype of these transgenic mice is due to the effect of desacyl ghrelin. Desacyl ghrelin has been shown not to activate GHS-R (39). There have been several reports saying that desacyl ghrelin has biological activities, such as promoting adipogenesis (41), inhibition of cell proliferation, inhibition of apoptosis (42), and counteracting the effect of *n*-octanoylated ghrelin (35).

We showed here that the ghrelin level in portal vein is significantly higher than that in retroorbital vein in wild type mouse. Ghrelin has been reported to be mainly synthesized in stomach and intestine. The step-up of plasma ghrelin level in gastric vein has been reported previously (43), but there has been no report showing the step-up of plasma ghrelin level in portal vein as compared with that in systemic circulation. The present study is the first report of the step-up of plasma ghrelin levels in portal vein. Moreover, the step-up of desacyl ghrelin in RIP-G Tg was much higher than that in control littermates, indicating overproduction of desacyl ghrelin by transgene in the pancreas.

The body weight, percent body fat, and food consumption of RIP-G Tg were not significantly different from those of nontransgenic littermates. Recently, we and Asakawa *et al.* have reported the studies of β -actin promoter ghrelin transgenic mouse (44, 45), in which plasma desacyl ghrelin levels were 30 and 50 times higher than those of their nontransgenic littermates. These transgenic mice were reported to show small phenotype, although some discrepancy of interpretation regarding on etiology exists. Asakawa *et al.* reported that the triglyceride level of β -actin promoter ghrelin transgenic mouse

was lower, but that cholesterol level and free fatty acid level were not changed compared with their nontransgenic littermates. The triglyceride levels of our RIP-G Tg only showed lower tendency compared with that of nontransgenic littermates. The lack of small phenotype and milder phenotype of lipid metabolism in RIP-G Tg may result from the fact that plasma desacyl ghrelin level of RIP-G Tg was only 3.4 times higher than those of nontransgenic littermates.

The tissue sections of the pancreas of these transgenic mice showed no apparent disarrangement in the islet architecture and in β cell mass. There have been several reports on the transgenic mice overexpressing humoral factors in the β cells, such as parathyroid hormone-related peptide, hepatocyte growth factor, and insulin-like growth factor-I (46–49). Some of these transgenic mice showed islet hypertrophy or disarrangement of the endocrine cells in the islet (46–49). Our observation showed that desacyl ghrelin might have no apparent effects on the islet architecture and β cell mass.

In the present study plasma insulin levels after the 3.0 g/kg glucose injection were significantly lower in RIP-G Tg than those in nontransgenic littermates, although there was no significant difference in plasma insulin levels between RIP-G Tg and nontransgenic littermates on the fasting state. To rule out the decreased production of insulin caused by exogenous insulin promoter, we measured insulin mRNA level and content in the pancreata of our transgenic mice. The insulin mRNA level and content from the transgenic mice were not significantly different from those from nontransgenic littermates. Therefore, the insulin production might not be disturbed in these mice either in transcriptional or translational levels. The immunoreactivity of PDX-1, which is the master regulator of the pancreas development and essential for insulin transcription, in RIP-G Tg β cell was not different from that in β cells of nontransgenic littermates. These results suggest that the suppression of glucose-stimulated insulin secretion in RIP-G Tg might not be due to the transcriptional dysregulation of insulin caused by injection of exogenous insulin promoter.

RIP-G Tg did not show decreased-insulin secretion in response to arginine. Arginine is known to stimulate insulin secretion by the mechanisms that are different from those used by glucose, although the detail remains controversial (50, 51). However, it seems certain that arginine somehow evoked Ca^{2+} influx into the β cell, and that leads to the exocytosis of insulin-containing vesicles (52, 53). So at least, the decreased insulin secretion in RIP-G Tg might not be due to disorders in exocytosis process. Egido (28) reported that ghrelin inhibits insulin secretion from rat pancreas in response to arginine *in vitro*, however, there has been no report on the effect of desacyl ghrelin on arginine-induced insulin secretion.

The immunoreactivity of GLUT2, glucose transporter in the pancreatic β cell, in RIP-G Tg β cells, was indistinguishable from that in the β cells of nontransgenic littermates. Although immunohistochemistry is not so suitable for quantitative analysis, at least no apparent decreased expression or disposition of GLUT2 in RIP-G Tg β cell exists. Chronic exposure to the high level of desacyl ghrelin may not influence on GLUT2 expression.

We performed a batch incubation study of RIP-G Tg islet. The insulin secretion from isolated islets of RIP-G Tg was indistinguishable from that of nontransgenic littermates. This finding indicates that insulin secretion was not affected by overexpression of ghrelin transgene *in vitro* but was affected *in vivo*. The different observations *in vitro* and *in vivo* may be explained by dilution of ghrelin produced by transgene with the incubation buffer. Alternatively, suppression of insulin secretion of RIP-G Tg was not due to the effect of desacyl ghrelin on

insulin secretion from β cell but on insulin sensitivity. Recently Gauna *et al.* (55) reported that co-administration of desacyl ghrelin and active ghrelin improves insulin sensitivity in humans (54) and that desacyl ghrelin suppress glucose output from liver. Although an insulin tolerance test did not show a statistically significant difference in blood glucose levels between RIP-G Tg and their nontransgenic littermates, there was a tendency for lower blood glucose levels of RIP-G Tg. Moreover, plasma triglyceride levels of RIP-G Tg showed lower tendency. Taken together, these results may indicate that desacyl ghrelin may improve insulin sensitivity of RIP-G Tg. The suppression of insulin secretion of RIP-G Tg is likely due to the effect of desacyl ghrelin on insulin sensitivity.

To explore if chronic exposure to high level desacyl ghrelin may influence the expression level of GHS-R, we investigated the mRNA level of GHS-R in the pancreas and pituitary of RIP-G Tg. No significant differences were found in GHS-R mRNA levels in pancreas or in pituitary between RIP-G Tg and their nontransgenic littermates. These findings indicate that chronic exposure to high level desacyl ghrelin might not influence the GHS-R mRNA expression level.

We also developed RGP-G Tg. The pancreatic tissue ghrelin concentrations determined by C-RIA of RGP-G Tg were about 50 times higher than those of their nontransgenic littermates, indicating that ghrelin was overexpressed in RGP-G Tg. However, there was no obvious phenotype regarding insulin secretion and pancreatic morphology. Considering the observation that portal ghrelin levels were not elevated in RGP-G Tg compared with those in their nontransgenic littermates, the amount of secreted ghrelin from α cell may not outstrip the amount from stomach.

In summary we developed RIP-G Tg, in which pancreatic desacyl ghrelin content was $\sim 1,000$ times higher than that in control littermates. We detected *n*-octanoylated ghrelin-like immunoreactivity in pancreatic β cells by immunohistochemistry, indicating that the mechanism of acylation may exist not only in pancreatic α cells but also in β cells. The glucose-stimulated insulin secretion of RIP-G Tg was decreased. There were no abnormalities with the arginine-induced insulin secretion, pancreatic histology, pancreatic insulin mRNA levels, and insulin content in the RIP-G Tg. The absence of insulin suppression in the islet batch incubation study, lower tendency of blood glucose levels in insulin tolerance test, and lower tendency of plasma triglyceride level may indicate that the suppression of insulin secretion of RIP-G Tg is likely due to the effect of desacyl ghrelin on insulin sensitivity. Although we also developed RGP-G Tg with a 50-fold increase of pancreatic desacyl ghrelin content, we did not find obvious phenotype regarding insulin secretion and pancreatic morphology. The present study raises the possibility that desacyl ghrelin may have an influence on glucose metabolism.

REFERENCES

- Kojima, M., Hosoda, H., Date, Y., Nakazato, M., Matsuo, H., and Kangawa, K. (1999) *Nature* **402**, 656–660
- Date, Y., Kojima, M., Hosoda, H., Sawaguchi, A., Mondal, M. S., Suganuma, T., Matsukura, S., Kangawa, K., and Nakazato, M. (2000) *Endocrinology* **141**, 4255–4261
- Gualillo, O., Caminos, J., Blanco, M., Garcia-Caballero, T., Kojima, M., Kangawa, K., Dieguez, C., and Casanueva, F. (2001) *Endocrinology* **142**, 788–794
- Mori, K., Yoshimoto, A., Takaya, K., Hosoda, K., Ariyasu, H., Yahata, K., Mukoyama, M., Sugawara, A., Hosoda, H., Kojima, M., Kangawa, K., and Nakao, K. (2000) *FEBS Lett.* **486**, 213–216
- Korbonits, M., Kojima, M., Kangawa, K., and Grossman, A. B. (2001) *Endocrine* **14**, 101–104
- Tena-Sempere, M., Barreiro, M. L., Gonzalez, L. C., Gaytan, F., Zhang, F. P., Caminos, J. E., Pinilla, L., Casanueva, F. F., Dieguez, C., and Aguilar, E. (2002) *Endocrinology* **143**, 717–725
- Asakawa, A., Inui, A., Kaga, T., Yuzuriha, H., Nagata, T., Fujimiya, M., Katsura, G., Makino, S., Fujino, M. A., and Kasuga, M. (2001) *Neuroendocrinology* **74**, 143–147
- Masuda, Y., Tanaka, T., Inomata, N., Ohnuma, N., Tanaka, S., Itoh, Z., Hosoda, H., Kojima, M., and Kangawa, K. (2000) *Biochem. Biophys. Res. Commun.* **276**, 905–908
- Shintani, M., Ogawa, Y., Ebihara, K., Aizawa-Abe, M., Miyanaga, F., Takaya, K., Hayashi, T., Inoue, G., Hosoda, K., Kojima, M., Kangawa, K., and Nakao, K. (2001) *Diabetes* **50**, 227–232
- Seoane, L. M., Tovar, S., Baldelli, R., Arvat, E., Ghigo, E., Casanueva, F. F., and Dieguez, C. (2000) *Eur. J. Endocrinol.* **143**, R7–R9
- Takaya, K., Ariyasu, H., Kanamoto, N., Iwakura, H., Yoshimoto, A., Harada, M., Mori, K., Komatsu, Y., Usui, T., Shimatsu, A., Ogawa, Y., Hosoda, K., Akamizu, T., Kojima, M., Kangawa, K., and Nakao, K. (2000) *J. Clin. Endocrinol. Metab.* **85**, 4908–4911
- Arvat, E., Di Vito, L., Broglio, F., Papotti, M., Muccioli, G., Dieguez, C., Casanueva, F. F., Deghenghi, R., Camanni, F., and Ghigo, E. (2000) *J. Endocrinol. Invest.* **23**, 493–495
- Date, Y., Murakami, N., Kojima, M., Kuroiwa, T., Matsukura, S., Kangawa, K., and Nakazato, M. (2000) *Biochem. Biophys. Res. Commun.* **275**, 477–480
- Date, Y., Nakazato, M., Murakami, N., Kojima, M., Kangawa, K., and Matsukura, S. (2001) *Biochem. Biophys. Res. Commun.* **280**, 904–907
- Nagaya, N., Uematsu, M., Kojima, M., Ikeda, Y., Yoshihara, F., Shimizu, W., Hosoda, H., Hirota, Y., Ishida, H., Mori, H., and Kangawa, K. (2001) *Circulation* **104**, 1430–1435
- Tschop, M., Smiley, D. L., and Heiman, M. L. (2000) *Nature* **407**, 908–913
- Wren, A. M., Small, C. J., Ward, H. L., Murphy, K. G., Dakin, C. L., Taheri, S., Kennedy, A. R., Roberts, G. H., Morgan, D. G., Ghatei, M. A., and Bloom, S. R. (2000) *Endocrinology* **141**, 4325–4328
- Nakazato, M., Murakami, N., Date, Y., Kojima, M., Matsuo, H., Kangawa, K., and Matsukura, S. (2001) *Nature* **409**, 194–198
- Inui, A. (2001) *Nat. Rev. Neurosci.* **2**, 551–560
- Date, Y., Nakazato, M., Hashiguchi, S., Dezaki, K., Mondal, M. S., Hosoda, H., Kojima, M., Kangawa, K., Arima, T., Matsuo, H., Yada, T., and Matsukura, S. (2002) *Diabetes* **51**, 124–129
- Volante, M., Allia, E., Gugliotta, P., Funaro, A., Broglio, F., Deghenghi, R., Muccioli, G., Ghigo, E., and Papotti, M. (2002) *J. Clin. Endocrinol. Metab.* **87**, 1300–1308
- Wierup, N., Svensson, H., Mulder, H., and Sundler, F. (2002) *Regul. Pept.* **107**, 63–69
- Wierup, N., Yang, S., McEvilly, R. J., Mulder, H., and Sundler, F. (2004) *J. Histochem. Cytochem.* **52**, 301–310
- Prado, C. L., Pugh-Bernard, A. E., Elghazi, L., Sosa-Pineda, B., and Sussel, L. (2004) *Proc. Natl. Acad. Sci. U. S. A.* **101**, 2924–2929
- Sun, Y., Ahmed, S., and Smith, R. G. (2003) *Mol. Cell. Biol.* **23**, 7973–7981
- Wortley, K. E., Anderson, K. D., Garcia, K., Murray, J. D., Malinova, L., Liu, R., Moncrieffe, M., Thabet, K., Cox, H. J., Yancopoulos, G. D., Wiegand, S. J., and Sleeman, M. W. (2004) *Proc. Natl. Acad. Sci. U. S. A.* **101**, 8227–8232
- Broglio, F., Arvat, E., Benso, A., Gottero, C., Muccioli, G., Papotti, M., van der Lely, A. J., Deghenghi, R., and Ghigo, E. (2001) *J. Clin. Endocrinol. Metab.* **86**, 5083–5086
- Egido, E. M., Rodriguez-Gallardo, J., Silvestre, R. A., and Marco, J. (2002) *Eur. J. Endocrinol.* **146**, 241–244
- Reimer, M. K., Pacini, G., and Ahren, B. (2003) *Endocrinology* **144**, 916–921
- Broglio, F., Gottero, C., Benso, A., Prodham, F., Destefanis, S., Gauna, C., Maccario, M., Deghenghi, R., van der Lely, A. J., and Ghigo, E. (2003) *J. Clin. Endocrinol. Metab.* **88**, 4268–4272
- Adeghate, E., and Pomery, A. S. (2002) *Neuroendocrinol.* **14**, 555–560
- Lee, H. M., Wang, G., Englander, E. W., Kojima, M., and Greeley, G. H., Jr. (2002) *Endocrinology* **143**, 185–190
- Salehi, A., Dornonville De La Cour, C., Hakanson, R., and Lundquist, I. (2004) *Regul. Pept.* **118**, 143–150
- Broglio, F., Benso, A., Gottero, C., Prodham, F., Gauna, C., Filtri, L., Arvat, E., van der Lely, A. J., Deghenghi, R., and Ghigo, E. (2003) *J. Endocrinol. Invest.* **26**, 192–196
- Broglio, F., Gottero, C., Prodham, F., Gauna, C., Muccioli, G., Papotti, M., Abribat, T., Van Der Lely, A. J., and Ghigo, E. (2004) *J. Clin. Endocrinol. Metab.* **89**, 3062–3065
- Iwakura, H., Hosoda, K., Doi, R., Komoto, I., Nishimura, H., Son, C., Fujikura, J., Tomita, T., Takaya, K., Ogawa, Y., Hayashi, T., Inoue, G., Akamizu, T., Hosoda, H., Kojima, M., Kangawa, K., Imamura, M., and Nakao, K. (2002) *J. Clin. Endocrinol. Metab.* **87**, 4885–4888
- Guz, Y., Montminy, M. R., Stein, R., Leonard, J., Gamer, L. W., Wright, C. V., and Teitelman, G. (1995) *Development* **121**, 11–18
- Thorens, B., Sarkar, H. K., Kaback, H. R., and Lodish, H. F. (1988) *Cell* **55**, 281–290
- Hosoda, H., Kojima, M., Matsuo, H., and Kangawa, K. (2000) *Biochem. Biophys. Res. Commun.* **279**, 909–913
- Herrera, P. L., Nepote, V., and Delacour, A. (2002) *Endocrine* **19**, 267–278
- Thompson, N. M., Gill, D. A., Davies, R., Loveridge, N., Houston, P. A., Robinson, I. C., and Wells, T. (2004) *Endocrinology* **145**, 234–242
- Baldanzi, G., Filigheddu, N., Cutrupi, S., Catapano, F., Bonissoni, S., Fubini, A., Malan, D., Baj, G., Granata, R., Broglio, F., Papotti, M., Surico, N., Bussolino, F., Isgaard, J., Deghenghi, R., Sinigaglia, F., Prat, M., Muccioli, G., Ghigo, E., and Graziani, A. (2002) *J. Cell Biol.* **159**, 1029–1037
- Murakami, N., Hayashida, T., Kuroiwa, T., Nakahara, K., Ida, T., Mondal, M. S., Nakazato, M., Kojima, M., and Kangawa, K. (2002) *J. Endocrinol.* **174**, 283–288
- Ariyasu, H., Takaya, K., Iwakura, H., Hosoda, H., Akamizu, T., Arai, Y., Kangawa, K., and Nakao, K. (2005) *Endocrinology* **146**, 355–364
- Asakawa, A., Inui, A., Fujimiya, M., Sakamaki, R., Shinfuku, N., Ueta, Y., Meguid, M. M., and Kasuga, M. (2005) *Gut* **54**, 18–24
- Garcia-Ocana, A., Takane, K. K., Syed, M. A., Philbrick, W. M., Vasavada,